
Integrate Analysis of MeRIP-seq and RNA-seq Reveals METTL14 as a Core Regulator of Follicular Granulosa Cell Development in Zi Geese

[Jinbo Zhao](#) , Jiaqiang Dong , Hong Zhang , Kun Yang , Mingdong Huo , Niandong Wei , Long Fu , Wenjiang Zhao , [Hongbao Wang](#) , [Zhigang Ma](#) * , [Zhifeng Chen](#) *

Posted Date: 14 May 2026

doi: 10.20944/preprints202605.0946.v1

Keywords: N⁶-methyladenosine modification; small yellow follicle; *METTL14*; granulosa cell



Preprints.org is a free multidisciplinary platform providing preprint service that is dedicated to making early versions of research outputs permanently available and citable. Preprints posted at Preprints.org appear in Web of Science, Crossref, Google Scholar, Scilit, Europe PMC, OpenAlex.

Copyright: This open access article is published under a [Creative Commons CC BY 4.0 license](#), which permit the free download, distribution, and reuse, provided that the author and preprint are cited in any reuse.

Disclaimer/Publisher's Note: The statements, opinions, and data contained in all publications are solely those of the individual author(s) and contributor(s) and not of MDPI and/or the editor(s). MDPI and/or the editor(s) disclaim responsibility for any injury to people or property resulting from any ideas, methods, instructions, or products referred to in the content.

Article

Integrate Analysis of MeRIP-seq and RNA-seq Reveals METTL14 as a Core Regulator of Follicular Granulosa Cell Development in Zi Geese

Jinbo Zhao ^{1,2}, Jiaqing Dong ¹, Hong Zhang ¹, Kun Yang ¹, Mingdong Huo ¹, Niandong Wei ¹, Long Fu ¹, Wenjiang Zhao ¹, Hongbao Wang ¹, Zhigang Ma ^{1,*} and Zhifeng Chen ^{1,2,*}

¹ Branch of Animal Husbandry and Veterinary of Heilongjiang Academy of Agricultural Sciences, Qiqihar 161005, China

² Postdoctoral Research Workstation of Heilongjiang Academy of Agricultural Sciences Agricultural Sciences, Harbin 150086, China

* Correspondence: mazhigang521521@163.com (A.M.); qqhr139@sina.com (Z.C.);

Tel.: 0452-6135219 (A.M.); qqhr139@sina.com (Z.C.); Fax: 0452-6135219 (A.M.); 0452-6135219 (Z.C.)

Highlights

What are the main findings?

- m⁶A methylation modification was widely distribution in small yellow follicle tissues of Zi geese, and 78 differentially methylation genes (DMGs) were identify in Healthy small yellow follicle and atresia small yellow follicle groups, these DMGs are involved in follicle growth and development.
- We revealed *METTL14* acts as a core regulator affecting steroid synthesis, proliferation and apoptosis in Zi geese follicle granulosa cells.

What are the implications of the main findings?

- The main findings point out the direction for further in-depth research on improving follicle development quality and egg production performance.
- These results provide a feasible theoretical basis for the industrial application of potential molecular targets for the genetic improvement of geese reproductive traits.

Abstract

m⁶A is a ubiquitous reversible post-transcriptional RNA methylation modification in eukaryotic cells, which has been positive effect on regulating follicles development in animals. However, the role of m⁶A modification profiling in regulating the development of healthy and atresia small yellow follicle have not yet been studied in poultry. In this study, we conducted a comparative analysis of the m⁶A methylation profiles of healthy and atresia follicles Zi goose during the period of peak egg-laying. Here, we discovered that 23,342 and 25,552 m⁶A peak between healthy small yellow follicles group (HSYF) and atresia small yellow follicle groups (ASYF), which were mainly enriched in 3'-UTR and stop codon regions. We found that 1174 differential upregulated peaks and 1250 differential downregulated peaks were identified in ASYF group, these differential peaks were covered 1141 and 1233 genes, including *METTL14*, *WTAP*, *IGF2BP3* and *CYTB*. Motif analysis demonstrated that these m⁶A peaks exhibit the RRACH and DRACH conserved consensus sequence. Importantly, Zi goose follicle transcriptome was extensively methylated and a positive correlation between the m⁶A peak and gene expression levels. The combined analysis of MeRIP-seq and RNA-seq revealed that a total of 78 DMGs were shared in HSYF and ASYF groups, such as *BMP5*, *PPARGC1A*, *NGF*, *SCD5*, which were mainly involved in TGF β signaling pathway, MAPK signaling pathway, PPAR signaling pathway and ECM receptor interaction. Furthermore, *METTL14* plays a regulatory role in Zi goose granulosa cell development, which was verified by in vitro experiments. We found that knockdown of *METTL14* dramatically prevented GCs apoptosis, promoted GCs proliferation, increased the production and secretion of steroid hormone, enhanced the expression levels of genes related to

steroid hormone synthesis in granulosa cell. Conversely, overexpression of *METTL14* resulted in opposite outcomes. Additionally, we also observed that knockdown of *METTL14* increased the activities of antioxidant enzyme (SOD, GSH and CAT), decreased the activities of MDA in goose GCs. Conversely, overexpression of *METTL14* inhibited the activities of antioxidant enzymes, increased the activities of MDA. In summary, these data collectively demonstrated that m⁶A methylation was widely distributed in the process of geese follicle growth and development, and further confirm the significant role of *METTL14* influences on granulosa cell development of Zi geese. These findings can be a considerable efficient way to facilitate the laying egg performance of Zi goose through molecular marker assisted breeding technology.

Keywords: N⁶-methyladenosine modification; small yellow follicle; *METTL14*; granulosa cell

1. Introduction

Egg production is a vital economic traits in poultry industry [1]. Zi geese, as an excellent indigenous goose breed resource in China, which is famous for its high egg production [2]. The level of egg production in poultry is directly influenced by the follicles development [3]. Follicle selection in poultry refers to the process of selecting a dominant follicle from the small yellow follicle pool development into hierarchical follicles, which is a key process influencing the egg production performance in poultry [4]. Ovarian follicles are composed of oocyte and its surrounding somatic cell, including granulosa cells (GCs) and thecal cells [5]. Previous studies have shown that granulosa cell play an important role in determining the fate of follicles [6], and apoptosis of granulosa cells lead to follicular atresia [7]. Apoptosis and autophagy of granulosa cell is closely associated with follicular atresia [8].

N⁶-methyladenosine modification (m⁶A), as ubiquitous reversible epigenetic modification of messenger RNA (mRNA), which regulates gene expression through post-transcriptional mRNA modifications [9], including the regulation of mRNA stability [10,11], splicing [12,13], and translation [14]. It has also been shown to be widely found in mRNAs, miRNAs and lncRNAs [15]. Aberrant m⁶A modification affect sex hormone synthesis, fertility and early embryonic development [16,17]. Recently studies have revealed that N⁶-methyladenosine modification plays crucial regulatory roles follicle development in multiple species. In porcine follicular atresia, knockdown of *METTL3* significant increase the mRNA expression level of Serine/threonine-protein kinase (ULK1), as well as the autophagy level [8], the m⁶A reader YTH domain-containing family member 2 (YTHDF2) mediates the effect of brain-derived neurotrophic factor (BDNF) on porcine follicular GCs proliferation [18]. In chicken study field, m⁶A may affect the egg production performance of Gushi chickens by altering the expression of genes related to follicular development, such as Wingless-type MMTV integration site family member 4 (WNT4), Anti-Mullerian Hormone (AMH), and Fibroblast growth factor 16 (FGF16) [19]. m⁶A modification of key factors in Wnt pathway could play a major role in regulating chicken follicle selection [20]. In cattle study field, m⁶A modification related to the regulation of ovarian ovulation and follicular development in the yak ovary [21]. These finding suggested that m⁶A modification may be involved in follicle development in animals.

Methylated RNA immunoprecipitation sequencing (MeRIP-seq) is a power technique to map m⁶A in a transcriptome-wide level [22]. Currently, MeRIP-seq was widely used in study fields of ovarian diseases, such as polycystic ovary syndrome [23], premature ovarian failure [24], and abnormal oogenesis [25]. However, the molecular regulatory network underlying the important economic trait of egg production in Zi geese from the perspective of N⁶-methyladenosine modification remains elusive.

In the present study, this work provided a comprehensive m⁶A methylation profile of Zi goose between healthy and atresia small yellow follicle, we aimed to mining m⁶A methylation modification peaks of functional genes, providing a new insights into understanding the process of follicle atresia development and improving the egg production performance.

2. Materials and Methods

2.1. Animals, Experimental Design and Sample Collection

A total of 280 laying Zi geese received from Branch of Animal Husbandry and Veterinary of Heilongjiang Academy of Agricultural Sciences Experimental Ranch (Latitude: 49°19'; Longitude: 123°45'; Altitude: 155m). All Zi geese were fed in the same housing environment, with the temperature maintained at 23±2°C, and the average relative humidity controlled at 60±5%. In this study, Zi geese enters peak egg-laying period, with egg production in the top 5% of the normal distribution were defined as the healthy small yellow follicle group (HSYFs), with an average egg production of 37.00±0.58, Zi geese with egg production in the lowest 5% of the normal distribution are defined as the atresia small yellow follicle group (ASYFs), and their average egg production was 5.25±0.48. Eight Zi geese at the same batch and similar body weight (3.1±0.35kg) were selected during the period of egg-laying between HSYF and ASYF groups. All selected Zi geese were euthanized by anesthesia with pentobarbital sodium and cervical dislocation. Subsequently, the ovaries tissue were collected at aseptic conditions and rinsed with 0.9% normal saline to separate small yellow follicles tissues. Health small yellow follicle (HSYF) and atresia small yellow follicle (ASYF) were collected based on the follicle size, morphology, the content of serum and follicle tissues hormones as previously described. These geese were fed standard commercial diets. The ingredients and compositions of all diets for Zi goose laying period are listed in Table 1.

Table 1. Dietary composition and nutrient levels for breeding geese.

Items	Amount
Dietary composition	
Corn (%)	536.00
Soybean meal (%)	210.00
CaCO ₃ (%)	12.00
Trace mineral premix compound (%)	2.00
Nacl	5.00
Sprayed corn bran	100.00
Compund vitamin premix (%)	0.40
Corn germ meal (%)	77.10
Feed phytase	0.20
60% Choline chloride	1.00
Limestone powder	55.00
DL-Met	0.90
50% Vitamin E	0.20
Feed mycotoxin binder	0.20
Nutrient levels	
ME(kcal/kg)	2601
CP (%)	17.06
Met (%)	0.31
Met+Cys (%)	0.54
Leu (%)	1.21
Arg (%)	1.01
Thr (%)	0.50
Trp (%)	0.15
Ile (%)	0.59
VaL (%)	0.75
His (%)	0.41
Phe (%)	0.71
C18:2	20.07
CF (%)	3.61

Ash (%)	9.86
Ca (%)	2.50
TP (%)	0.62

Abbreviations: ME: metabolizable energy; CP: crude protein; Met: methionine; Cys: cystine; Lys: lysine; Arg: arginine; Thr: threonine; Trp: tryptophan; CF: crude fiber; Ash: crude ash; Ca: calcium; TP: total phosphorus.

2.2. Measurement of Reproductive Hormones Concentration in Serum and SYF Tissue

The blood samples were centrifuged at 3000 r/min for 15 minutes to separate serum and were frozen at -20°C , add an appropriate amount of physiological saline to the tissue and homogenize it. Centrifuge the sample at 3000r/min for 10 minutes, and then collect the supernatant to analyze the levels of LH, E2, FSH and P4. These hormones were measured with commercial ELISA kits (Jiangsu Mei mian industrial Co., Ltd., Taizhou, China) in accordance with the manufacturer's instructions.

2.3. Hematoxylin-Eosin Staining in Healthy and Atresia Follicles

Small yellow follicle (6-8mm) tissue samples were collected, and immediately fixed in 4% paraformaldehyde, dehydrated, embedded in wax, and then cut into 4 μm thick sections, and hematoxylin and eosin staining were performed. Morphology of healthy and atresia follicles were observed using Case Viewer software, granalosa cell layer thickness were measured using saiviewer software. Small yellow follicle granulosa cells apoptosis was detected using the Tunel assay. Green-positive area of the granulosa cell layer was employed using Aipathwell software.

2.4. RNA Extraction, Library Construction and Sequencing

Total RNA was extracted and purified from each small yellow follicle sample with TRIzol following the manufacturer's instructions. The concentration and quality of RNA were determined using NanoDrop ND-1000 (NanoDrop,) The integrity of the RNA was carried out an Agilent 2100 Bioanalyzer (Aligent Santa Clara,CA,USA) with a RIN>9.5. Ploy (A) RNA was isolated from total RNA using an Dynabeads Oligo. We obtained the m⁶A transcriptome profile map of Zi geese healthy and atresia small yellow follicle development were detected by MeRIP-seq. The sample RNA was fragmented into approximately 100 nt fragments, The RNA was divided into two different groups. One group was used for the input control experiment (without Immunoprecipitation experiments were performed), which was directly employed for generating the transcriptome sequencing library. The other group was enriched with m⁶A specific antibody. After capturing the m⁶A-modified RNA, the antibody elution was performed using magnetic beads to reduce the background noise associated with non-specific binding. After library construction was completed, the quality of all the libraries were performed using an Agilent Bioanalyzer 2100 system (Agilent Technology, Inc., Santa Clara, CA, USA). the quality-checked libraries(Gene Denovo Biotechnology Co., Ltd., Guangzhou, China) were sequenced on the NovaSeq 6000 platform.

2.5. Bioinformatics Analysis of MeRIP-seq and RNA-seq Data

The Fastp software was employed to screen the raw data, which included the removal of containing adapter, duplicate sequences, and low quality reads so as to obtain clean reads. The Bowtie2 (version: 2.2.8) tool was utilized to map the high quality clean reads onto the ribosomal database of geese. Subsequently, the read segments that aligned to ribosomal RNA were excluded. The clean reads were aligned to the goose reference genome (Taihu goose T2T genome) using HISAT2 (version: 2.1.0) software. The R package exome Peak2 was used to screen peak calling on genome scale, MEME and HOMER software was employed to detect the significant sequence motif in the transcript sequence associated with peaks and perform motif analysis. The differential m⁶A peaks based on the criteria of $|\log_2(\text{fold change})| \geq 1$ and $p\text{-value} < 0.05$ between HSYF and ASYF groups were evaluated. StringTie software were employed to perform gene assemble, and FPKM was

employed to calculate the expression levels of all genes in HSYF and ASYF groups samples. The differentially expressed genes (DEGs) were identified using the R package DESeq2, and DEGs based on the criteria of $|\log_2(\text{fold change})| > 1.5$ and $p\text{-value} < 0.05$ between HSYF and ASYF groups. Meanwhile, using clusterProfiler, Gene Ontology (GO) and Kyoto Encyclopedia of Genes and Genomes (KEGG) functional enrichment analysis were carried out on the genes associated with the differential peaks and discovered DEGs. Furthermore, Joint analysis of differentially expressed methylated peaks (DEPs) ($|\log_2(\text{fold change})| \geq 1$, $p\text{-value} < 0.05$) and differentially expressed genes (DEGs) ($|\log_2(\text{fold change})| \geq 1$, $p\text{-value} < 0.05$) between the HSYF and ASYF groups were performed. The plot results were visualized using the ggplot2 R package.

2.6. Reverse Transcription Real-Time Quantitative (RT-qPCR)

To confirm the accuracy of our analysis, qPCR was used to detect the differentially expressed genes expression level, including BMP5, PPARGC1A, NGF, and SCD5. Total RNA was extracted from healthy and atresia small yellow follicle groups, The concentration and purity of total RNA were detected using the Nanodrop2000. The mRNA was reversed transcribe into cDNA using 5×SweScript All-in-One Super Mix with gDNA remover for qPCR. Reverse transcription real-time quantitative (RT-qPCR) was employed using 2×Universal Blue SYBR Green qPCR master mix. All reactions were performed in triplicate, and the relative mRNA expression abundance was normalized by the $2^{-\Delta\Delta C_t}$ method. The β -actin was used as the internal reference gene, and the details of gene specific primers sequences are presented in Table 2.

Table 2. Specific primer sequences for RT-qPCR.

Gene	Gene BankAccession	Primer Sequences (5'→3')	Size (bp)
CYP11A1	XM_048081523.2	F: GCTTCGCTCTGGAGTCTGTG R: ATGTA CTCCCTGCTGCTCTTTGC	286
StAR	XM_013194444.3	F: TCCAGAAATCGCTCAGCATCC R: AATCTTGACCTCTTTGACGCTGG	221
CYP17A1	XM_013174485.3	F: CACCGAACACAAGGAAGCCT R: GAGCACAGTCCACTTGAGCA	202
CYP19A1	XM_067003805.1	F: TGGTCCTGGTCTCGTGCGTAT R: TTGCCAAGCATCAAAGTAGTTCTG	217
METTL14	XM_048066298.2	F: GTCTGGATCTTGGCCGAGTG R: GCAGTGCTCCTTGGTTCTTTG	146
WTAP	XM_048067845	F: CTAATGATGTGACGGGATTGA GAGA R: TCCACCATTGTTGATCGCAGT	247
FTO	XM_048075341	F: CTTGGCCTACTGAGGGTTATGA AAT R: CCTTGTAATGCCTTGACTGCTTC	118
ALKBH5	XM_066977782.1	F: AGTTCCAGTTCAAGCCCATCA G R: CTA CT CAGCGATTTCGTTTCCA	205

YTHDF1	XM_066978553.1	F: TACCATCGTGGACGGACAAA R: CACGAGGTTGGTTTAGATACTGG	225
YTHDF2	XM_066982731.1	F: AAGGGACGTTTTGATGTCAGG T R: CTCCTGGCGTTTTCATAGTGT	222
YTHDF3	XM_048061722.2	F: TCAGGGACAATCAACGCAAAG R: CATATCTCCACCGATTTTCAGTCC	178
IGF2BP3	XM_066991829.1	F: GAAAGAAGGAGCAACCATCA GA R: CTCAGGAGTTGAGTGGATGGTAA	119
BMP5	XM_048078086.2	F: GCAGAGGGATACGGAAAGGA R: CGGCTGCTGTCACTGCTTCT	264
PPARGC1A	XM_048046820.2	F: TACAGCAATGAACCCGCCAAT A R: ATCTCCATCTGTCAGTGCATCAAAC	144
NGF	XM_066983081.1	F: CCCAAATCCCACCAGAGTAAC R: ACCGAAACGCTTCTTCTTAAA	145
SCD5	XM_066996639.1	F: TCGTGCTGATGTGCTTTGTGAT R: GAGGATGGAGGCAAGGAAGTAG	92
β -actin	XM_013174886.1	F: AATCAAGATCATTGCCCCGC R: TAATCCTGAGTCAAGCGCCAAA	268

Abbreviations: forward primer (F), reverse primer (R), cytochrome P450 family 11 subfamily A member 1 (CYP11A1), cytochrome P450 family 19 subfamily A member (CYP19A1), cytochrome P450 family 17 subfamily A member 1 (CYP17A1), steroidogenic acute regulatory protein (StAR), fat mass and obesity associated (FTO), methyltransferase 14 (METTL14), WT1 associated protein (WTAP), insulin like growth factor 2 mRNA binding protein 3 (IGF2BP3), alkylation repair homolog protein 5 (ALKBH5), YTH domain family, member 1 (YTHDF1), YTH domain family, member 2 (YTHDF2), YTH domain family, member 3 (YTHDF3), bone morphogenetic protein 5 (BMP5), PPARG coactivator 1alpha (PPARGC1A), nerve growth factor (NGF), stearyl-CoA desaturase 5 (SCD5).

2.7. Cell Culture and Transfection

Geese granulosa cell (GCs) were isolated and cultured as previously described [26]. Briefly, the prehierarchical follicles (6-8mm in diameter) was obtained from peak laying period of Zi goose, and then washed with chilled PBS for three times, the granulosa cell layers was extracted within chilled PBS and pipette repeatedly to release air bubbles, the tissues were subjected to digestion with 0.28% trypsin and 2mg/ml tpye IV collagenase for 30min at 37°C. The digestion process was terminated by adding complete medium supplemented with 10% Fetal Bovine Serum and the resulting mixture was filtered through 70 μ m cell strainer to remove yolk clumps and tissue fragments. The cells were gently overlaid onto 2 ml of 50% Percoll and centrifuged at 2500rpm for 20 min, the white membranous cell

layer at the interface were harvested resuspended in 1ml PBS and mixed thoroughly by pipetting. Subsequently, these culture plates were placed in a CO₂ incubator, with the culture conditions maintained at 37°C with 5% CO₂.

Three si-METTL14 sequences were designed and synthesized by Sybio Technologies Co., Ltd., (Suzhou, China). The coding sequence of the goose METTL14 gene (Genbank accession XM_048066298.2) were amplified by PCR and inserted into *Nhe* I and *Hind* III restriction sites of pcDNA3.1(+) vector plasmid. The constructed METTL14 overexpression vector was confirmed by DNA sequencing. According to the manufacturer's instructions, the si-METTL14 and OE-METTL14 transfection was performed with Lipofectamin™3000 reagent (Invitrogen, USA). After transfection for 48h, the granulosa cell from each groups were collected for subsequent experiments.

2.8. FSHR Immunofluorescence Assay

Geese GCs were cultured in 6-well plates and washed with PBS for three times. Subsequently, cell were fixed with 4% paraformaldehyde for 10 minutes, permeabilized with 0.2% TritonX-100 for 5 minutes, and blocked with 5% bovine serum albumin (BSA) for 30 minutes. Cell were then incubated with a FSHR antibody overnight at 4°C. After washing with PBS, cells were incubated with Goat anti-Rabbit IgG H&L for 1h at 37°C. Nuclei were counterstained with DAPI, fluorescent image were captured using a fluorescent microscope, and the relative fluorescent intensity of FSHR was analyzed using Image J software.

2.9. Cell Proliferation Assay

Cell proliferation was performed using an 5-ethynyl-2'-deoxyuridine (EdU) assay. Briefly, Geese GCs were cultured in 6-well plates and transfection with *overexpression-METTL14* and *sh-METTL14* for 48h. Cells were then incubated with EdU working solution at 37°C for 2h. Subsequently, cell were fixed in 4% paraformaldehyde for 15min and permeabilization with 0.3% Triton X-100 for 10 minutes, Nuclei were stained with 4',6'-diamidino-2-phenylindole (DAPI) for 10 minutes. The granulosa cell proliferating were determined using Image J software, and the proliferation ratio were calculated as the percentage of EdU-positive to total DAPI-positive cells.

2.10. Flow Cytometry Analysis

Geese granulosa cell were cultured in a 6-well cell culture plates, followed by transfected with *overexpression-METTL14* and *sh-METTL14* for 48h, and washed twice with phosphate buffered saline (PBS). For cell apoptosis detection, cell were resuspended in binding buffer and stained with Annexin V-FITC and propidium iodide (PI) according to the manufacturer's protocol (Novel Biotech), followed by incubation in the dark for 15 minutes at 37°C. For cell cycle analysis, cell were fixed in 70% ethanol at -20°C overnight, washed with PBS, and stained with PI staining solution containing RNase A (Novel Biotech). The flow cytometry analysis were conducted using BD AccuriC6 flow cytometer (BD Biosciences).

2.11. Enzyme Linked Immunosorbent Serologic Assay

Granulosa cell isolated from geese were cultured in a 6-well cell culture plates, followed by transfected with *overexpression-METTL14* and *sh-METTL14* for 48h. Subsequently, the medium was collected from the 6-well plates, centrifuge at 2500r/pm at 4°C for 5 minutes and subjected to reproductive hormone concentration and oxidative stress index analysis using luteinizing hormone (LH), follicle-stimulating hormone (FSH), progesterone (P4), superoxide dismutase (SOD), malondialdehyde (MDA), Glutathione (GSH), catalase (CAT) ELISA kits from Fine Biotech (Wuhan, China).

2.12. Western Blotting Analysis

Total protein was extracted from granulosa cell in each group and then subjected to 10% SDS-PAGE followed by transfer to PVDF membrane, the membrane was incubated at 4°C overnight with

the following primary antibodies targeting: PCNA (10205-2-AP, Proteintech, 1:1000), Caspase3 (19677-1-AP, Proteintech, 1:1000), Caspase8 (13423-1-AP, Proteintech, 1:1000), BAX (50599-2-Ig, Proteintech 1:1000), BCL2 (12789-1-AP, Proteintech, 1:1000), StAR (bs-3570RP, Bioss, 1:1000), CYP11A1 (13363-1-AP, Proteintech, 1:1000), CYP17A1 (14447-1-AP, Proteintech, 1:1000), CYP19A1 (NBP1-45360, NOVUS, 1:1000). Goat Anti-Rabbit IgG HRP (IS0001, Affinity, 1:10000) and Goat Anti-mouse IgG HRP (IS0002, Affinity, 1:10000) were used for secondary antibodies with incubating for 2h at room temperature. The protein bands were visualized by ECL chemiluminescence. GAPDH was referred as the internal reference protein.

2.13. Statistical Analysis

The data obtained in our experiment were analyzed using the Graph Pad Prism 9.0 software. All data were expressed as means \pm standard error of the mean (SEM) and were analyzed using Student's *t*-test, and at least three replicates were performed in our experiment. Bar with *, **, *** represent $p < 0.05$, $p < 0.01$, $p < 0.001$ significance levels, respectively.

3. Results

3.1. Reproductive Hormones Concentrations, Morphological Characteristic Observation of Follicles, and Apoptosis Assay Analysis

As shown in Figure 1A and 1B, four healthy individuals from HSYF and ASYF groups were randomly selected during the period of laying for sample collection, Among them, the granulosa layer of small yellow follicles were observed and scanned under the microscope using the SaiViewer software. Blood and SYF tissue collection were determined the concentration of follicle stimulating hormone (FSH), luteinizing hormone (LH), Progesteron (P₄) and estradiol (E₂) using enzyme linked immunosorbent assay. TUNEL assay was performed the granulosa cell of apoptosis. As can be seen in the Figure 2A, the concentration of FSH, LH, and E₂ were extremely significant higher in the serum of the HSYF group than that in the ASYF group ($P < 0.0001$), a significant higher of P₄ was found in the serum of the HSYF group compared with ASYF group ($P < 0.001$). To investigate the impact of reproductive hormone on the small yellow follicle development, the concentration of reproductive hormones in the small yellow follicle tissues were measured (Figure 2B), we found that the concentration of FSH, LH, and P₄ of HSYF group were extremely significant higher than that ASYF group ($P < 0.0001$), the concentration of E₂ in HSYF group than those ASYF group ($P < 0.001$). These findings collectively suggest that the concentration of reproductive hormone in serum and SYF tissue are involved in regulating follicle development of Zi geese.

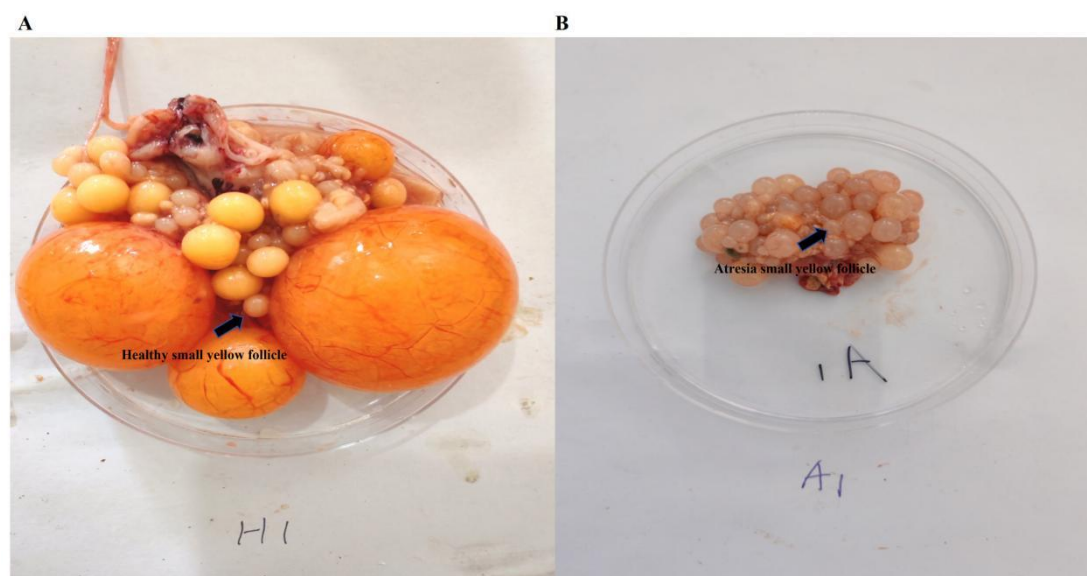


Figure 1. External morphology of the healthy follicle and atresia follicles. (A) Healthy follicle tissues of Zi goose. (B) Atresia follicles tissues of Zi goose. Black arrow point to healthy and atresia small yellow follicles.

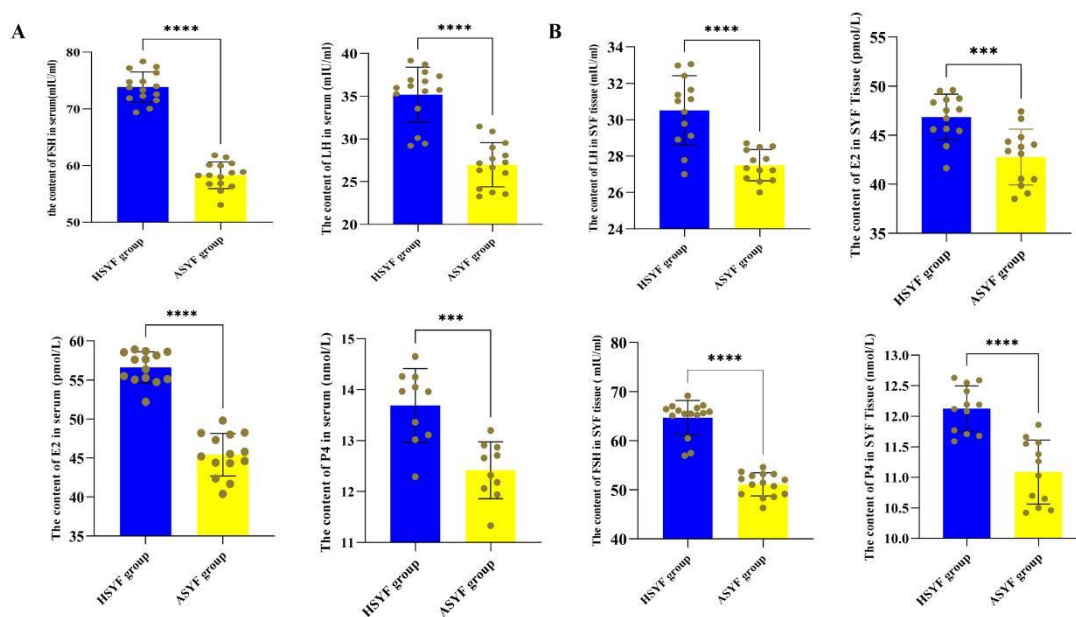


Figure 2. Determination of reproductive hormone secretion levels in serum and small yellow follicle tissues of Zi goose. (A) Reproductive hormone secretion levels in serum. (B) Reproductive hormone secretion levels in small yellow follicle tissues. * $p < 0.05$, indicating significance compared to HSYF group; ** $p < 0.01$, indicating extreme significance compared to HSYF group. *** $p < 0.001$, indicating extreme significance between HSYF and ASYF groups. Data are expressed as mean \pm SEM ($n=10$). Abbreviation: FSH: follicle stimulating hormone; LH: luteinizing hormone; E2: estradiol; P4: progesterone.

Granulosa cells, as crucial somatic cells, which is intricately associated with follicle development of poultry [27,28]. The H&E staining results showed that the SYF tissue of HSYF group exhibited granulosa cell intact structure, arranged closely, and without obvious structural deficiencies (Figure 3). As can be seen in the Figure 4, tunnel assay results showed that the granulosa cell green positive area of HSYF and ASYF groups was no significant difference ($P > 0.05$). In terms of the thickness granulosa cell layers of HSYF and ASYF groups, the thickness granulosa cell layers of HSYF group was significantly higher than that ASYF group ($P < 0.001$), with a diameter of 11.6 μm -15.5 μm (Figure 4). Our data demonstrated that the essential role of granulosa cell are directly involved in the small yellow follicle development.

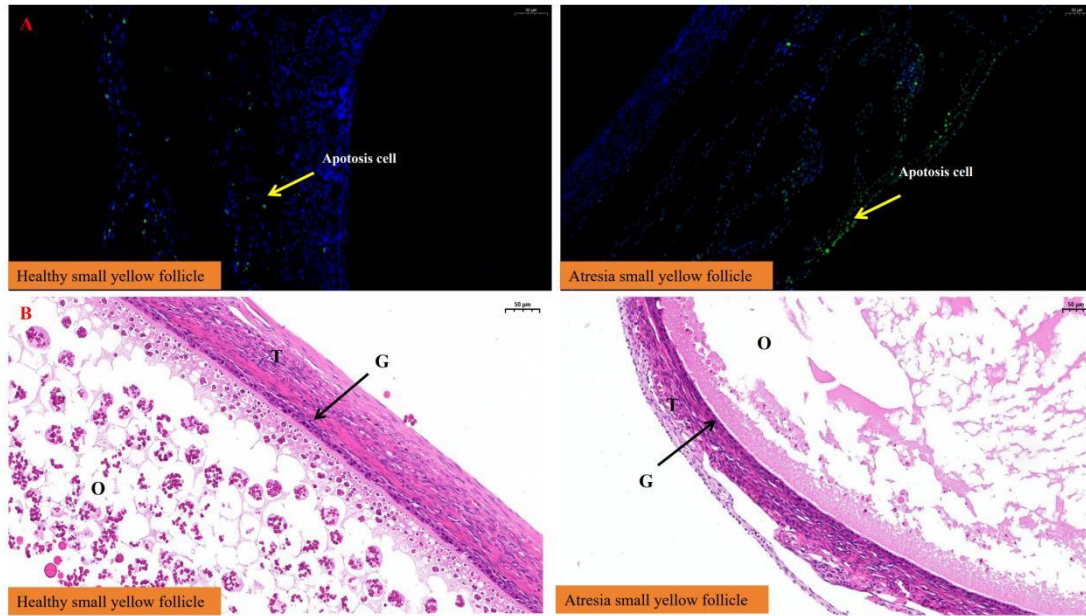


Figure 3. Results of tunnel assay and hematoxylin and eosin (H&E) staining between healthy small yellow follicles (HSYF group) and atresia small yellow follicles (ASYF group). (A) Tunnel assay of SYF tissue of Zi goose. (B) Hematoxylin and eosin (H&E) staining of SYF tissue of Zi goose. T: thecal layer; G: granulosa layer; O: oocytes. The Figures were imaged at 20x magnification. Yellow arrows point to apoptosis granulosa cell, the green positive area in the image indicate apoptosis granulosa cells.

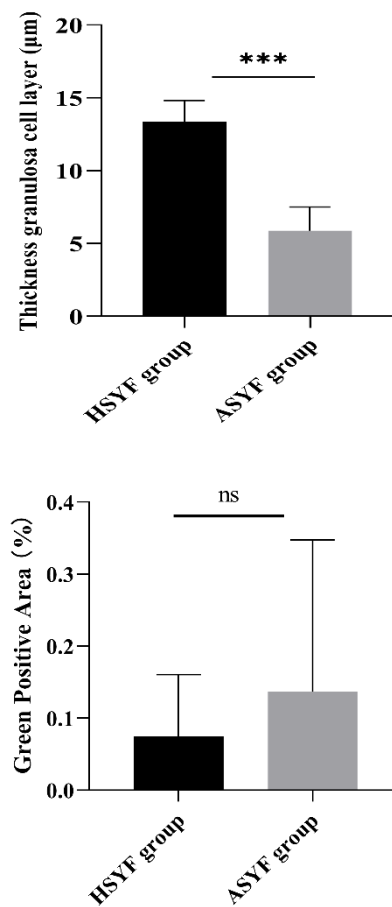


Figure 4. Measurement of granulosa cell layer thickness and green positive area. *** $p < 0.001$, indicating extreme significance compared to HSYF group, ^{ns} $p > 0.05$, indicating no significance between HSYF and ASYF groups. Data are expressed as mean \pm SEM ($n=5$).

3.2. Analysis of Genes Associated with Steroid Hormone Synthesis and m^6A Enzyme Expression Level in Goose syf Tissue

Steroid hormone synthesis genes, such as StAR, CYP11A1, CYP17A1, and CYP19A1, which plays a significant role in regulating follicle development by enhancing the synthesis of steroid hormones in granulosa cells [29]. As shown in Figure 5, we found that the mRNA expression levels of StAR, CYP17A1 and CYP11A1 in the HSYF group were significantly higher than those in the ASYF group ($P < 0.05$; $P < 0.01$), the mRNA expression levels of CYP19A1 was no significantly between HSYF and ASYF groups ($P > 0.05$).

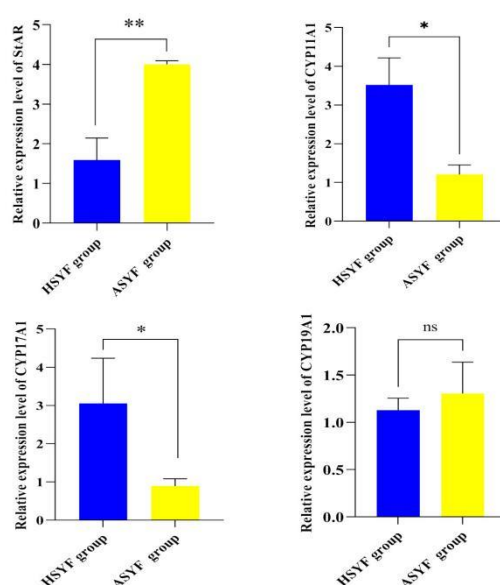


Figure 5. The expression levels of steroid hormone synthesis genes between HSYF and ASYF groups. * $p < 0.05$, indicating significance compared to HSYF group; ** $p < 0.01$, indicating extreme significance compared to HSYF group. ^{ns} $p > 0.05$, indicating no significance between HSYF and ASYF groups. Data are expressed as mean \pm SEM ($n=4$).

Emerging evidences suggest that m^6A modification enzyme has been shown to play a vital role in many reproductive processes, such as differentially m^6A methylated genes are associated with steroidogenesis and folliculogenesis in pig [30]. Hence, we investigated the impact of m^6A methylation genes on healthy and atresia small yellow follicle of Zi geese. As can be seen in Figure 6, the relative expression levels of METTL14 was extremely significantly lower in the HSYF group than those in the ASYF group ($P < 0.001$), the relative expression levels of IGF2BP1 gene was significantly higher in ASYF group than that in the HSYF group ($P < 0.05$). However, the relative expression level of YTHDF1 was significantly higher in the HSYF group than that in the ASYF group ($P < 0.05$). Interestingly, the relative expression levels of YTHDF2, YTHDF3, FTO, and WTAP genes was no significant difference between HSYF group and ASYF groups ($P > 0.05$). Our data demonstrated that m^6A methylation enzyme may play a regulatory role in regulating follicle growth and development.

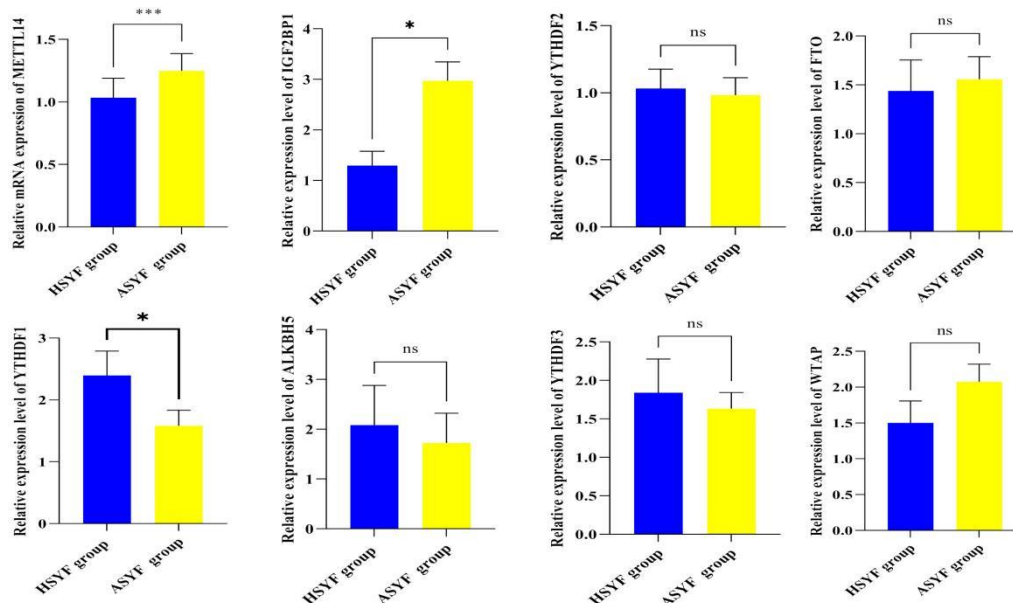


Figure 6. The expression levels of m^6A methylation genes between HSYF and ASYF groups. * $p < 0.05$, indicating significance compared to HSYF group; *** $p < 0.001$, indicating extreme significance compared to HSYF group. ns $p > 0.05$, indicating no significance between HSYF and ASYF groups. Data are expressed as mean \pm SEM ($n=4$).

3.3. Overview of the m^6A Methylation Profile in Small Yellow Follicles Development

To investigate the m^6A transcriptome map of follicle development in Zi goose, the healthy small yellow follicle (HSYF) and atresia small yellow follicle (ASYF) of Zi goose were performed on MeRIP-seq.

MeRIP-seq produced averages of 96329156 and 101408918 raw reads from IP sample between HSYF and ASYF groups. After filtering out low-quality data, 69010240 to 100747688 clean reads from each sample were mapped to Taihu_goose_T2T_genome Primary Assembly reference genome (NC_089876.1). More than 80% clean reads from all the sample were uniquely mapped to reference genome, suggesting that each sample has high-quality data available for subsequent analysis. As shown in Figure 7A, B, C, the m^6A peaks in HSYF group were mainly enriched in 3'-UTR (31.49%), stop codon (28.81%), coding DNA sequence (CDS) region (26.45%), followed by start codon (4.95%), and 5'-UTR (2.33%). In the ASYF group, the m^6A peaks were mainly enriched in 3'-UTR (28.19%), stop codon (28.67%), coding DNA sequence (CDS) region (28.61%), followed by start codon (6.10%), and 5'-UTR (2.46%). The results of enrichment scores of m^6A peaks in different gene functional elements indicated that the m^6A peaks were markedly enriched in the 3'-UTR region. Among gene functional elements, the percentage of m^6A peaks located in stop codon region was the most prominent, which suggested that m^6A peaks may be involved in regulating mRNA stability, and affecting the function of the 3'UTR of mRNA during small yellow follicles development of Zi goose. (Figure 7B, C).

As shown in Figure 7D, m^6A peaks is distributed across the *Anser cygnoides* genome between the two groups. To further determine the m^6A peaks contained in each transcript, we found that nearly 40% of the transcripts in the two groups contained only one m^6A modification peak, and the majority of genes contained 1-4 m^6A modification peaks.

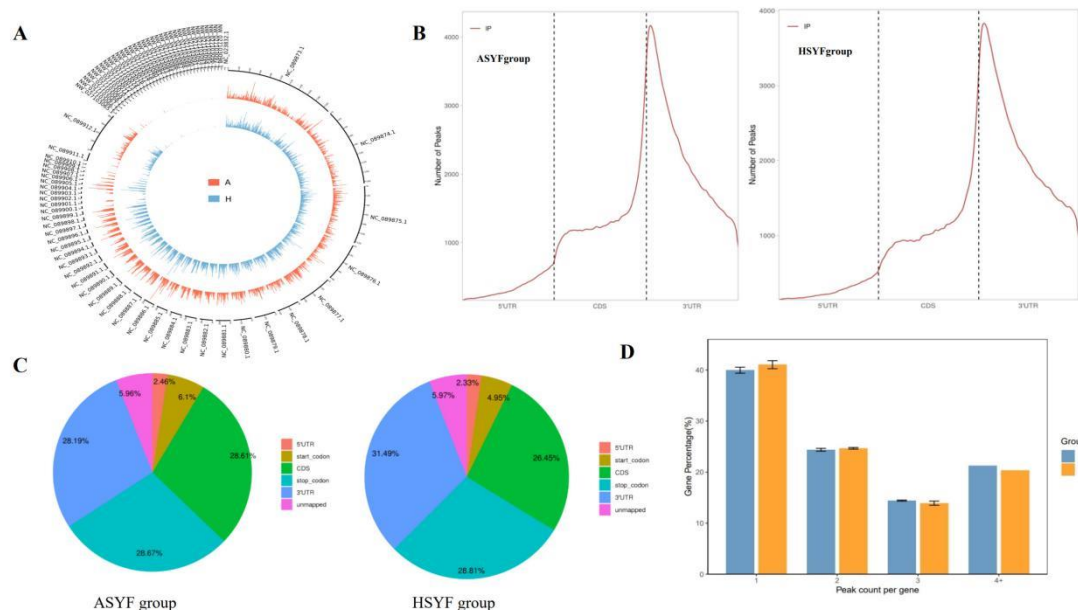


Figure 7. m^6A transcriptome map of healthy small yellow follicle and atresia small yellow follicle in Zi goose. (A) The distribution of m^6A peaks sits in Taihu_goose_T2T genome primary assembly reference between HSYF and ASYF groups. (B) Distribution of peaks relative to gene positions. (C) Distribution of peaks across different gene functional elements between HSYF and ASYF groups. (D) The diagram of peak count statistics between HSYF and ASYF groups.

The volcano plot showed that the distribution of differentially m^6A peaks, we identified 23342 and 25552 m^6A peaks in healthy and atresia small yellow follicle tissue in Zi geese. A total of 1174 differential upregulated peaks and 1250 differential downregulated peaks were identified in the HSYF and ASYF groups, these differential peaks were covered 1141 and 1233 genes (Figure 8A, B), suggesting that m^6A methylation peaks in small yellow follicles tissue is relatively richer. We found that some genes are related to follicular development, such as METTL14, SCD5, BMP5, NGF, WTAP, PPARGC1A. 17321 m^6A peaks overlapped between the two groups, including 6021 specific m^6A peaks in HSYF group and 8231 specific m^6A peaks in ASYF group (Figure 8C), suggesting the significant differences in m^6A modifications in the HSYF and ASYF groups. The m^6A methylation modification is highly conserved and usually embedded in 5'-RRACH-3' and 5'-DRACH-3' conserved consensus sequences, therefore, we performed a comprehensive motif scan analysis on healthy and atresia small yellow follicle in Zi geese m^6A peaks, As shown in Figure 8D, we found that GGACA was significantly enriched in the HSYF and ASYF groups, which suggested m^6A methylation modification was the most common post-transcriptional modification in animal. To better understand the functional differentially methylation genes (DMGs) in small yellow follicle development, GO and KEGG enrichment analyses were performed to investigate the role of DMGs in regulating follicles development of Zi geese. The GO analysis revealed that all the DMGs were mainly enriched in cell part, cell, intracellular, intracellular part, cytoplasm, plasma membrane processes. KEGG enrichment analysis revealed that all the DMGs were mainly involved in focal adhesion, lysine degradation, ECM receptor interaction, regulation of actin cytoskeleton, glycosaminoglycan biosynthesis, and sphingolipid metabolism signaling pathway (Figure 8E, F). These significantly enriched pathways may be associated with granulosa cell proliferation, and steroid hormone synthesis during the follicles growth and development.

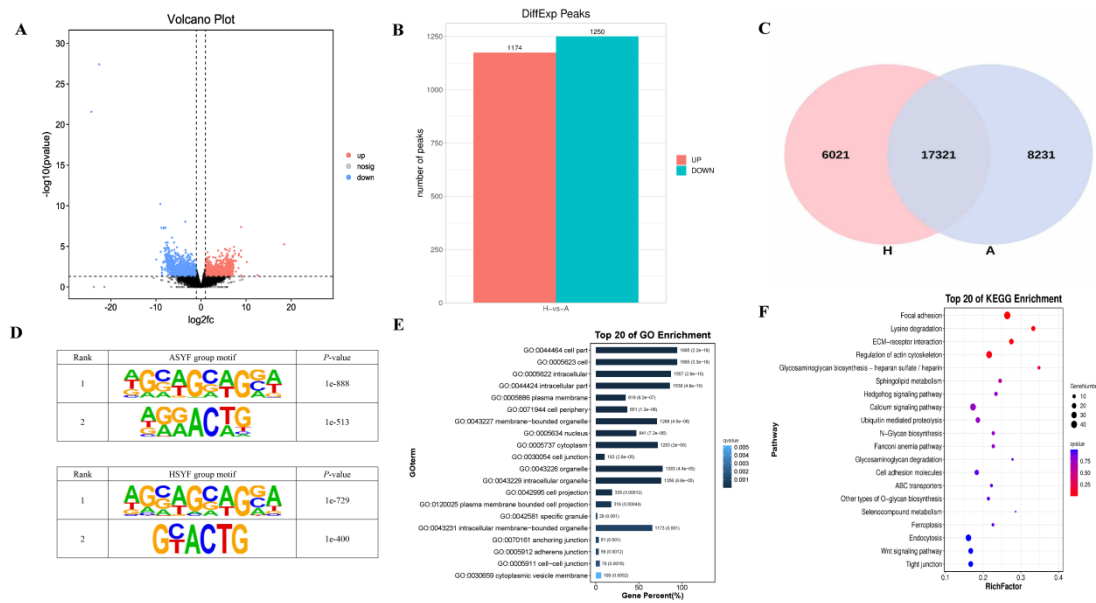


Figure 8. Analysis of differential m⁶A methylation of healthy small yellow follicle (HSYF group) and atresia small yellow follicle (ASYF group) in Zi geese. (A) The volcano plot of differentially m⁶A methylated genes (Red dots represent differentially upregulated methylation peaks; Blue dots represent differentially downregulated methylation peaks). (B) Number of differential up/down m⁶A peaks. (C) Number of common and specific m⁶A peaks of HSYF and ASYF groups in Zi geese. (D) Frequency distribution of the RRACH conserved consensus sequence motif across all peaks. (E) GO enrichment analysis of genes associated with peaks in HSYF and ASYF groups. (F) KEGG enrichment analysis of genes associated with peaks in HSYF and ASYF groups.

3.4. Identification of Differentially Expressed Genes via RNA Sequencing

In our study, Figure 9A, B revealed that a total of 775 genes were identified in ASYF group compared with HSYF group, including 207 up-regulated DEGs and 568 down-regulated DEGs, these DEGs included gonadotropin releasing hormone receptor (GnRHR), 5-hydroxytryptamine receptor 1 (HTR1), bone morphogenetic protein 5(BMP5), stearoyl-CoA desaturase 5(SCD5), PPARG coactivator 1alpha (PPARGC1A), and insulin like growth factor 2(IGF2). The gene expression abundance of all samples are shown in Figure 9C. To further reveal the functions of DEGs, GO and KEGG functional enrichment were performed, In biological process category, we found that the DEGs were mainly enriched in cellular process, biological process, metabolic process and regulation of biological process, In cellular component category, we found that the DEGs were associated with cell, cell part, organelle, and membrane, In molecular function category, we found that the DEGs were involved in binding, catalytic activity, molecular function regulator, and transcription regulator activity (Figure 9D,E). The findings of the KEGG enrichment analysis indicated that there was significant enrichment of differentially expressed genes in several signaling pathways associated with steroid biosynthesis, follicle development, such as, neuroactive ligand receptor interaction, phagosome, cell adhesion molecules, fatty acid metabolism, fatty acid biosynthesis, insulin signaling pathway, and PPAR signaling pathway (Figure 9D,E).

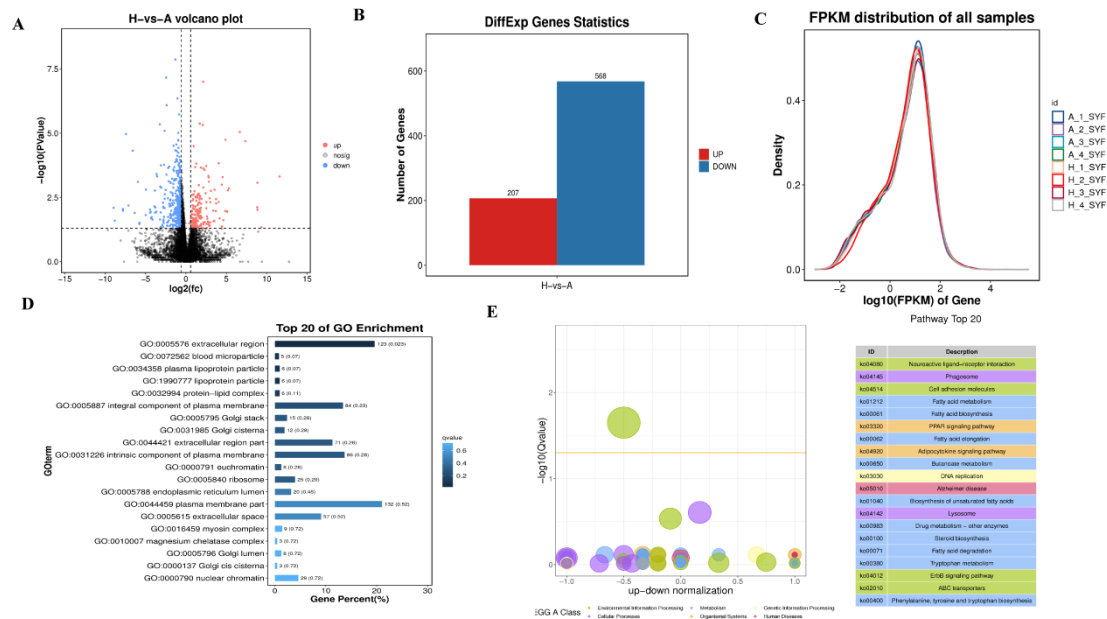


Figure 9. Results of Transcriptome Analysis between HSYF and ASYF groups. (A) Volcano plot of differentially expressed genes between HSYF and ASYF groups. (B) Number of differentially expressed genes. (C) FPKM distribution of HSYF and ASYF groups. (D, E) GO and KEGG analysis of differentially expressed genes.

3.5. Correlation Analysis of m⁶A Methylation and Differentially Expressed Genes

To investigate the association between m⁶A methylation modification and genes expression, we performed a joint analysis of MeRIP-seq and RNA-seq to explore the effect of m⁶A methylation modification on gene expression. As shown in Figure 10A, the overall expression levels of mRNAs with m⁶A modifications were higher than those of mRNAs without m⁶A modifications between HSYF and ASYF groups. Hence, we speculated that m⁶A methylation modification positively regulates mRNA expression. As shown in Figure 10B, C, The four quadrant diagram and venn diagram revealed that a total of 78 genes were identified as significantly co-differentially expressed genes in ASYF group relative to the HSYF group, including 184 hypermethylated DMGs (10 upregulated mRNAs and 174 downregulated mRNAs) and 90 hypomethylated DMGs (5 upregulated mRNAs and 85 downregulated mRNAs). The nine quadrant diagram revealed that 52 hypermethylated DMGs were identified, including 10 upregulated mRNAs and 42 downregulated mRNAs, 35 hypomethylated were identified, including 5 upregulated mRNAs and 30 downregulated mRNAs (Figure 10D). We found that the three genes related to small yellow follicles development, such as BMP5, NGF, SCD5 in ASYF group were significantly downregulated m⁶A levels compared to HSYF group. The transcription levels of BMP5, NGF, SCD5 were significantly downregulated in ASYF group than those in HSYF group. Interestingly, we found that the mRNA PPARGC1A was significantly higher m⁶A levels in ASYF group compared to the HSYF groups, while the transcription levels of PPARGC1A was significantly downregulated compared to the HSYF groups. Together our data indicated that the growth and development of small yellow follicles are controlled by the regulation of gene expression through m⁶A methylation modification.

To determine the specific functions of co-differentially expressed genes, we conducted GO and KEGG functional enrichment. In terms of biological process, we found that these DMGs were mainly annotated to cellular process, metabolic process, biological regulation; In terms of cellular component, these DMGs were mainly annotated to cell, cell part, membrane; In terms of molecular function, these DMGs were mainly annotated to binding, catalytic activity, and transporter activity (Figure 10E). KEGG analysis revealed that these DMGs were significantly enriched in neuroactive ligand receptor interaction, MAPK signaling pathway, mTOR signaling pathway, ECM receptor interaction, Wnt signaling pathway, Notch signaling pathway, TGF β signaling pathway,

and calcium signaling pathway (Figure10F). These significantly enriched pathways may be played an important role in steroid hormone biosynthesis, follicle growth and development. The findings suggested that m⁶A modification is predominantly involved in the developmental process of small yellow follicles, influencing the physiological process of follicle selection in geese.

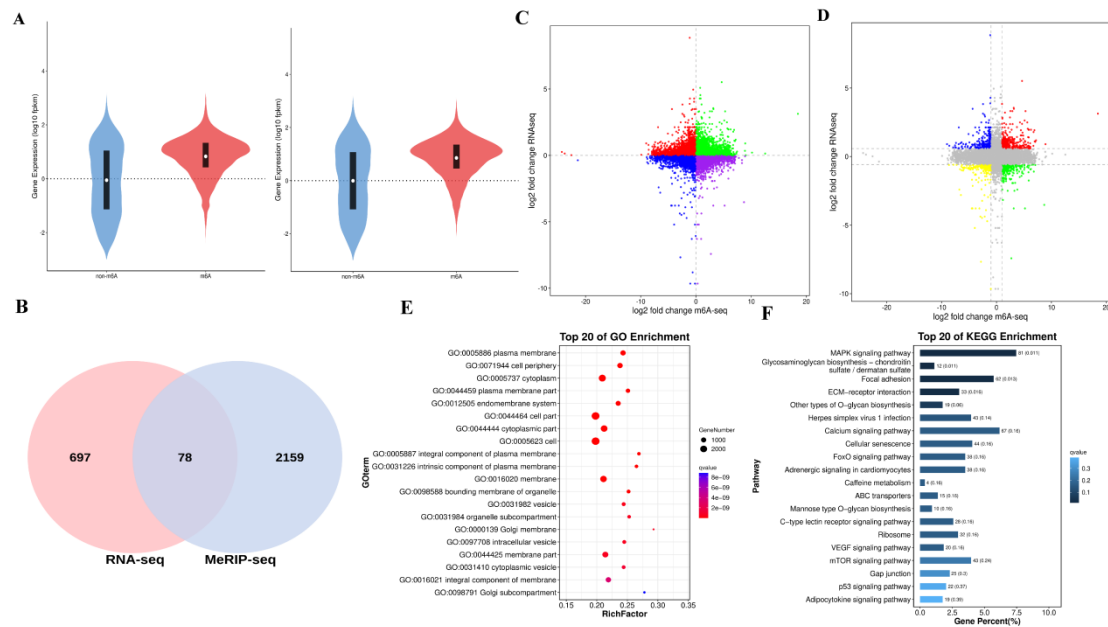


Figure 10. The integrated analysis results of RNA-seq and MeRIP-seq. (A) Violin plots of the expression of with / without m⁶A modification genes. (B) Venn diagram of co-differentially expressed genes by RNA-seq and MeRIP-seq. (C) The four quadrant diagram of MeRIP-seq and RNA-seq conjoint analysis. (D) The nine quadrant diagram of MeRIP-seq and RNA-seq conjoint analysis. (E, F) GO and KEGG analysis of differentially expressed methylated genes.

To validate the accuracy of the sequencing results, we employed quantitative real-time polymerase chain reaction (qPCR) to assess the consistency between the mRNA expression levels of four key genes and the transcriptome data. As shown in Figure 11, our results suggested that the expression of four key genes at qPCR level were consistent with the expression trends at the transcriptional level, which further verified the accuracy of the transcriptome sequencing results.

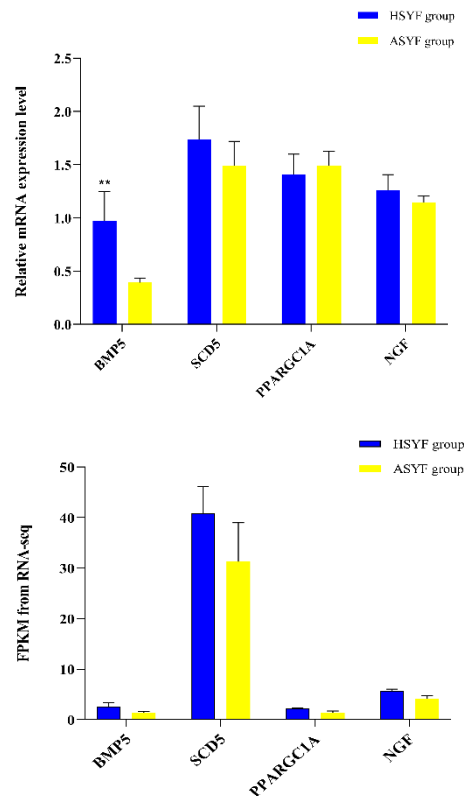


Figure 11. The qPCR and transcriptome profiling results of BMP5, SCD5, PPARGC1A, and NGF genes between HSYF and ASYF groups. (A) Results of quantitative detection of qPCR. (B) Results of transcriptome sequencing.

3.6. The essential Role of m⁶A Methylation writer *METTL14* in Follicular Granulosa Cells Development of Zi Geese

In this study, we found that 2424 differential m⁶A methylation peaks were identified in ASYF groups compared to HSYF group, these differential m⁶A methylation peaks covered 1141 and 1233 genes, including *METTL14*, *WTAP*, *IGF2BP3*, suggesting that m⁶A methylation genes plays crucial roles in regulating follicular development. Simultaneously, we integrated the quantitative expression data of m⁶A methyltransferase genes in healthy and atresia small yellow follicles, we found that the expression level of the *METTL14* genes in atresia small yellow follicle tissues was extremely significantly higher than that in healthy small yellow follicle tissues, implying that the *METTL14* genes plays a positive role in promoting follicular atresia. Subsequently, *METTL14* was identified as a key gene, and its functional verification was performed at the level of follicular granulosa cells in Zi geese.

To further investigate the essential role of m⁶A methylation writer *METTL14* in follicular granulosa cell of Zi geese, we performed a series of granulosa cell level validation experiments to elucidate the biological functions of *METTL14*. Follicle stimulating hormone receptor (FSHR) is a protein specifically expressed in follicle granulosa cell of female animals. In this study, We employed fluorescence in situ hybridization (FISH) to identify the isolated granulosa cells, and the granulosa cells expressing FSHR fluorescent protein exhibited a rhomboidal morphology. These findings indicated that granulosa cell were only cell that expressed FSHR (Figure 12A).

To investigate the functional role of *METTL14* genes in granulosa cell development, we constructed *METTL14* overexpression vector and synthesized three shRNAs (*sh-METTL14-1*, *sh-METTL14-2*, and *sh-METTL14-3*). RT-pPCR data revealed that overexpression *METTL14* group (*OE-METTL14*) was significantly higher than those OE vector group ($P < 0.01$). As shown in Figure 12B, *sh-METTL14* significantly reduced the expression level of *METTL14* in goose follicular granulosa cells, among them, *sh-METTL14-2* was the lowest the expression of *METTL14* ($P < 0.001$).

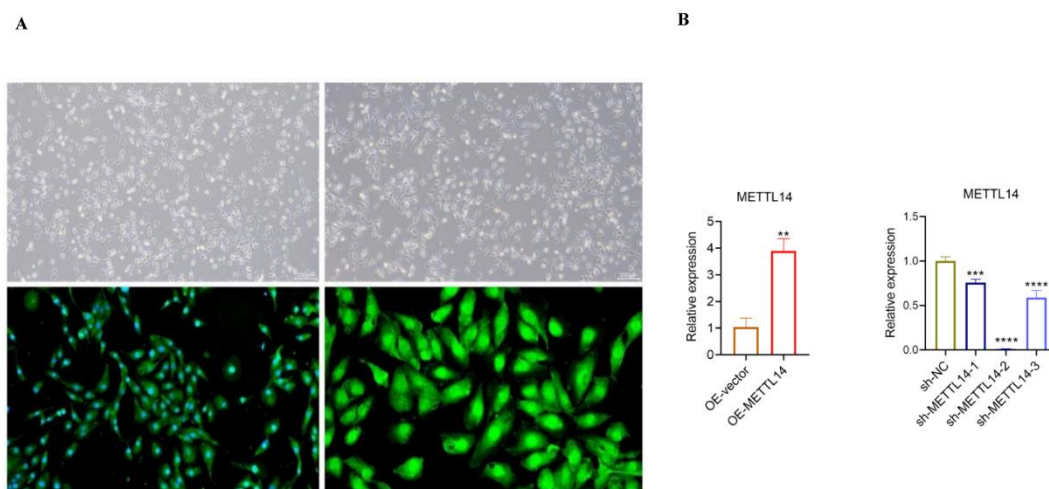


Figure 12. Culture of granulosa cells from Zi geese small yellow follicles, Immunohistochemical detection of FSHR, and verification of transfection efficiency. (A) Granulosa cell culture and immunohistochemical detection. (B) Verification of *METTL14* overexpression and knockdown efficiency in Zi geese granulosa cells. Data are expressed as mean±SEM ($n=4$), * $p<0.05$, ** $p<0.01$, *** $p<0.001$, **** $p<0.0001$.

3.7. Effect of *METTL14* on the Proliferation and Apoptosis of Zi Goose Follicular Granulosa Cell

The effect of *METTL14* on Zi geese follicular GCs proliferation and apoptosis was examined by EdU assays and flow cytometric analysis. As shown in Figure 13A and 13B, knockdown of *METTL14* significantly increased the proliferation of GCs at 48h compared to *sh-NC* group ($P<0.001$), overexpression of *METTL14* significantly reduce the proliferations of GCs at 48 h ($P<0.001$). As shown in Figure 13C and 13D, knockdown of *METTL14* significantly inhibited the apoptosis of GCs at 48h compared to *sh-NC* ($P<0.01$), overexpression of *METTL14* significantly promoted the apoptosis of GCs at 48h ($P<0.001$).

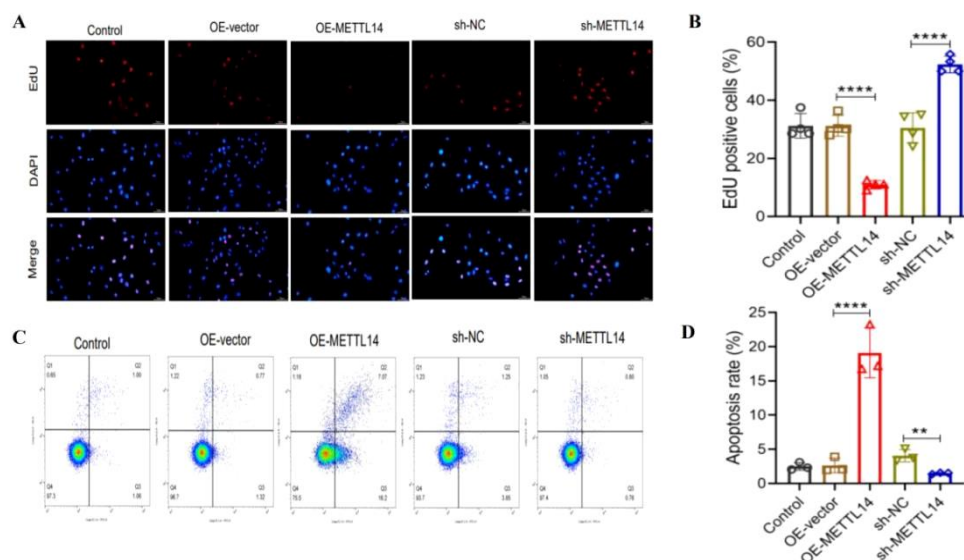


Figure 13. Effect of *METTL14* on proliferation and apoptosis of goose granulosa cell. (A,B) The proliferation rate of GCs with overexpression and knockdown of *METTL14* was assessed by EdU assay. (C, D) The apoptosis rate of GCs with overexpression and knockdown of *METTL14* was assessed by flow cytometry assay. Data are expressed as mean±SEM ($n=3$), * $p<0.05$, ** $p<0.01$, *** $p<0.001$, **** $p<0.0001$.

Furthermore, we also investigated the effect of *METTL14* on granulosa cell collected at 48 after transfection by determining cell apoptosis with flow cytometry. The flow cytometry analysis revealed that the percentage of cells cycle in the S phase was 35.3%, while that in the G2 phase was 14.6% at 48 hours following transfection with the *OE-METTL14* group, suggesting *OE-METTL14* arrested the transition of GCs from the S phase into G2/M phase. Conversely, the percentage of cells cycle in the S phase was 22.6%, and the G2 phase percentage was 21.8% at 48 hours after transfection with *sh-METTL14* group (Figure 14). These findings collectively highlight knockdown of *METTL14* may be played a vital role in preventing apoptosis of goose follicular granulosa cell.

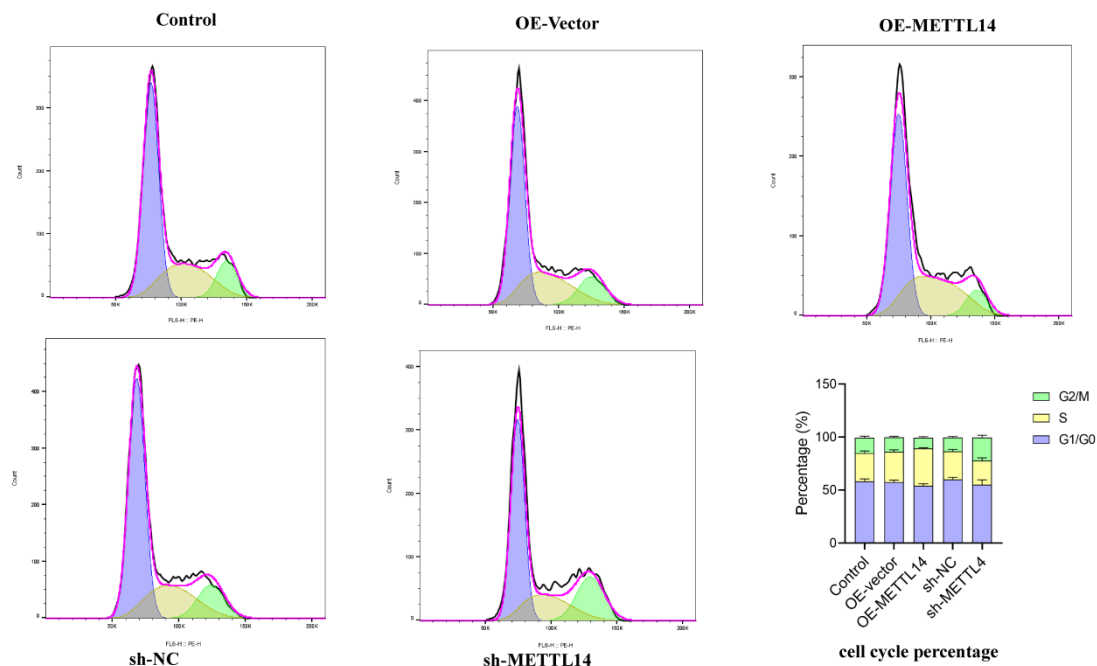


Figure 14. The cell cycle distribution in goose GCs analyzed by flow cytometry. G1: Gap 1 Phase, S: Synthesis Phase, G2: Gap 2 Phase. Data are expressed as mean \pm SEM ($n=3$), * $p<0.05$, ** $p<0.01$, *** $p<0.001$, **** $p<0.0001$.

As shown in Figure 15, western blotting analysis revealed that knockdown of *METTL14* significantly increased the protein expression levels of antiapoptotic proliferation cell nuclear antigen (PCNA), B cell lymphoma-2 (BCL2) ($P<0.05$; $P<0.01$). Conversely, overexpression of *METTL14* significantly increased the protein expression of apoptosis-promoting BCL2 associated X protein (BAX), caspase 3 and caspase 8 ($P<0.01$; $P<0.001$). These results showed that knockdown of *METTL14* promotes granulosa cell proliferation as well as inhibited granulosa cell apoptosis at protein level.

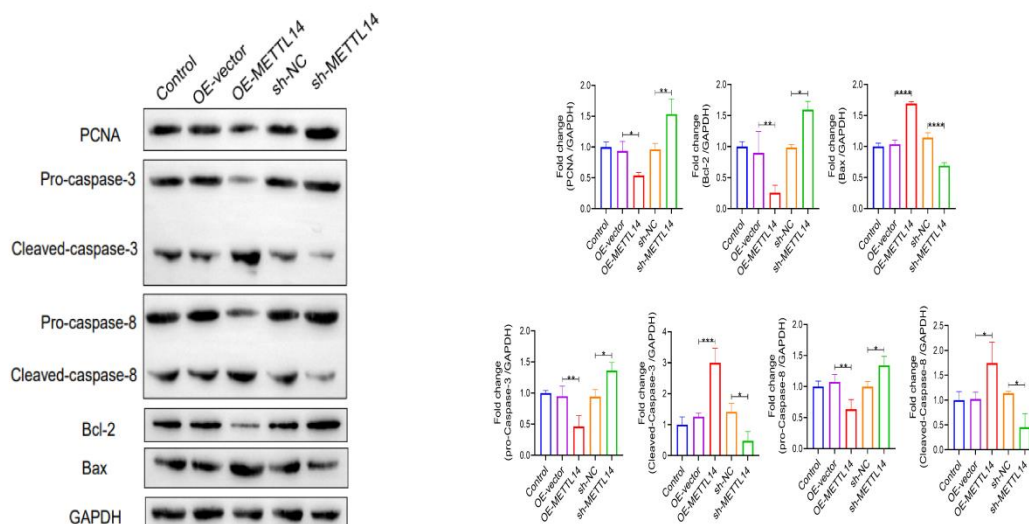


Figure 15. The protein expression levels of PCNA, caspase 3, caspase 8, BCL2 and Bax after knockdown or overexpression of *METTL14* in geese granulosa cells. Data are expressed as mean±SEM ($n=3$), * $p<0.05$, ** $p<0.01$, *** $p<0.001$, **** $p<0.0001$.

3.8. Effect of *METTL14* on the Steroid Hormone Production and STERIOD hormone Synthesis Related Genes of Zi Geese Follicular Granulosa Cell

The above findings collectively suggested that *METTL14* played a critical role in regulating the proliferation and apoptosis of granulosa cells. We further investigated the effect of *METTL14* on the steroid hormone synthesis and secretion of GCs. ELISA results showed that overexpression of *METTL14* in geese GCs significantly reduced the production and secretion of follicle stimulating hormone, progesterone compared to OE-vector group ($P<0.001$; $P<0.0001$), knockdown of *METTL14* in goose GCs increased the production and secretion of FSH, P4, and LH compared to *sh-NC* group ($P<0.001$; $P<0.0001$; Figure 16). These results indicated that RNA methyltransferase “writer” *METTL14* were involved in regulating the production and secretion of steroid hormones in Zi geese GCs. Several studies have suggested that steroid hormones, such as estrogen and progesterone produced by granulosa cells in poultry are directly regulated by steroid synthesis-related genes, which mainly included *StAR*, *CYP11A1*, *CYP17A1* and *CYP19A1*. Therefore, we further employed RT-PCR and western blotting techniques to determine the mRNA and protein expression levels of steroid hormone-related genes in granulosa cells. The results of RT-qPCR assay showed that knockdown of *METTL14* in goose GCs significantly increased the expression of gene related to follicle development and the synthesis of steroid hormones, including steroidogenic acute regulatory protein (*StAR*), cytochrome P450 family 11 subfamily A (*CYP11A1*), cytochrome P450 family 19 subfamily A (*CYP19A1*), and cytochrome P450 family 17 subfamily A (*CYP17A1*). Conversely, overexpression of *METTL14* in goose GCs significantly repressed the mRNA expression levels of *StAR*, *CYP11A1*, *CYP19A1*, and *CYP17A1* ($P<0.001$; $P<0.0001$; Figure 17A).

Furthermore, western blotting assay showed that the protein expression levels of *StAR*, *CYP11A1*, *CYP19A1*, and *CYP17A1* were consistent with the expression trends detected by RT-qPCR ($P<0.05$; $P<0.01$; Figure 17B, C). These findings collectively suggest that *METTL14* regulate the production and secretion of steroid hormone by altering the expression levels of steroid hormone-related genes of granulosa cells, thereby affecting goose follicles growth and development.

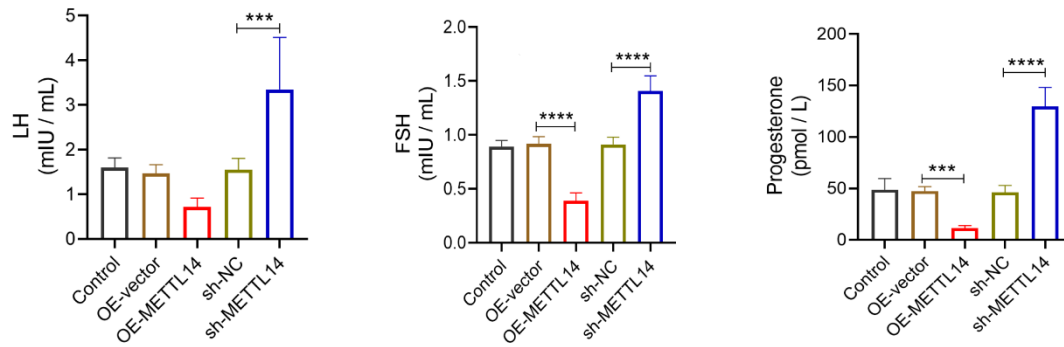


Figure 16. Overexpression and knockdown of *METTL14* affects the synthesis and secretion of steroid hormones in Zi geese GCs. Data are expressed as mean±SEM ($n=4$), * $p<0.05$, ** $p<0.01$, *** $p<0.001$, **** $p<0.0001$.

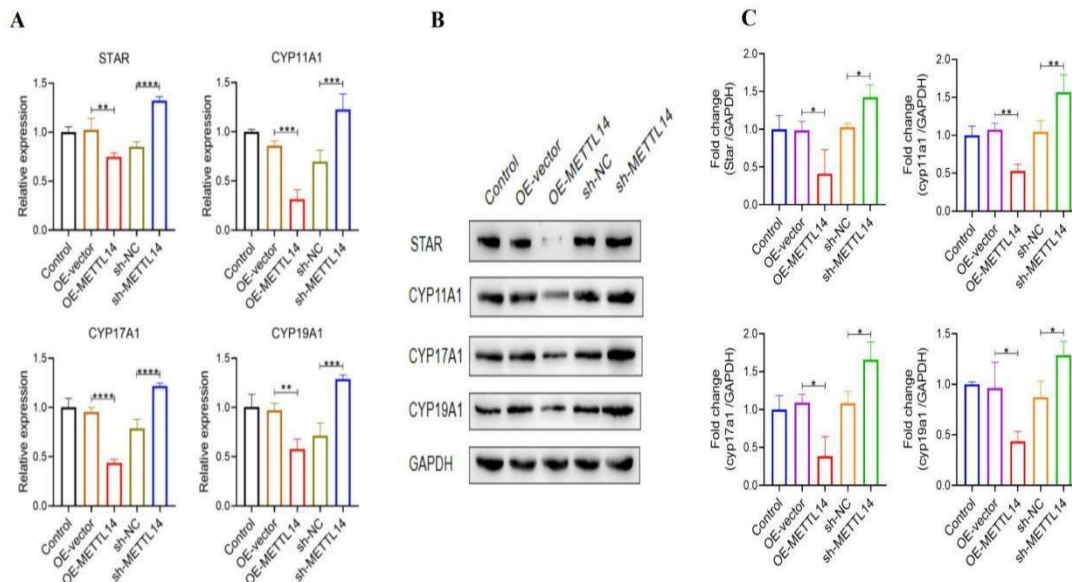


Figure 17. Overexpression and knockdown of *METTL14* modulates the expression of steroid hormone related genes in Zi geese GCs. (A) The relative mRNA expression of StAR, CYP11A1, CYP17A1, and CYP19A1 in geese GCs. (B,C) The protein expression levels of StAR, CYP11A1, CYP17A1, and CYP19A1 in geese GCs. Data are expressed as mean±SEM ($n=4$), * $p<0.05$, ** $p<0.01$, *** $p<0.001$, **** $p<0.0001$.

Oxidative stress has emerged as a critical factor in follicle atresia and ovarian aging [31], follicle atresia induced by oxidative stress is considered to be associated with apoptosis and autophagy of GCs [32,33], ELISA was used to examine knockdown and overexpression of *METTL14* influence on antioxidant enzymes (CAT, SOD, MDA and GSH). As shown in Figure 18, we found that overexpression of *METTL14* in geese GCs extremely significantly decreased the activities of CAT, SOD and GSH than in OE-vector group. Overexpression of *METTL14* in geese GCs increased the activities of MDA ($P<0.001$; $P<0.0001$). Conversely, the knockdown of *METTL14* in geese GCs extremely significantly increased the activities of SOD, GSH and CAT, but decreased the activities of MDA compared to *sh-NC* group ($P<0.001$; $P<0.0001$), implying that *sh-METTL14* can effectively prevent oxidative stress induced granulosa cell injury.

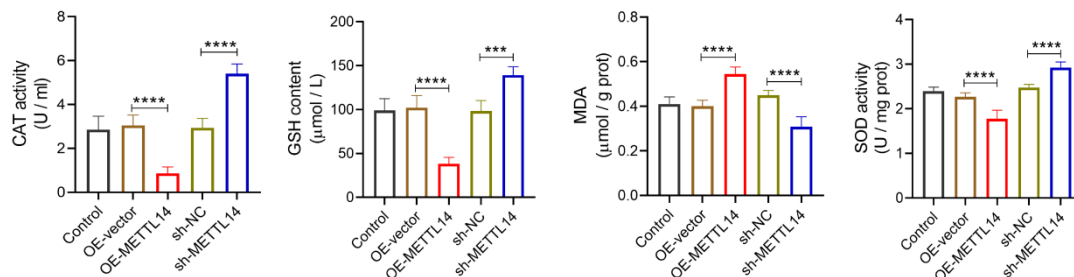


Figure 18. Effect of *METTL14* knockdown and overexpression on oxidative stress index of Zi geese granulosa cells. Data are expressed as mean±SEM ($n=4$), * $p<0.05$, ** $p<0.01$, *** $p<0.001$, **** $p<0.0001$.

4. Discussion

Egg production, as the most important economic traits in poultry industry, which directly affects goose farms economic benefits [34,35], and follicle development in poultry are strongly associated with egg production [36]. Numerous studies have demonstrated that follicle selection in poultry refers to a process of selecting dominant prehierarchical follicles (small yellow follicle, 6-8mm in diameter) for development into hierarchical follicles (12-15mm), and finally ovulation, which is an important process affecting egg performance in poultry industry [4]. Small yellow follicle represents a important developmental stage in poultry reproductive field, which has attracted growing attention from researchers [37]. To better understand the phenotypic differences between the HSYF (EN: 37.00) and the ASYF groups (EN: 5.25), the reproductive hormone contents of the serum and small yellow follicle tissues of Zi geese in the HSYF and ASYF groups were performed, as well as the mRNA expression of steroid synthase associated with genes *StAR*, *CYP11A1*, *CYP19A1*, and *CYP17A1* in small yellow follicle tissue was determined. Previous research has shown that the synthesis of P4 requires the combined action of *StAR* and *CYP11A1* [38], among them, *StAR* mediates the transport of cholesterol, followed by *CYP11A1* catalyzes the conversion of cholesterol to pregnenolone [39]. In our study, we found that the concentration of FSH, LH, P4, E2 of serum and follicle tissue in HSYF group extremely significantly higher than those that ASYF group, meanwhile, the mRNA expression level of *StAR*, *CYP11A1*, *CYP17A1* in HSYF group was significantly higher than that ASYF group, suggesting the content of serum and ovary tissue reproductive hormone, and steroid synthase related to gene expression level of small yellow follicle tissue were directly involved in follicles development.

m^6A methylation is the most prevalent internal modification in eukaryotic RNA [40], it has been demonstrated to play a crucial role in diverse biological and reproductive processes, including regulated early embryonic development of females [41,42], testosterone production of testicular leydig cell [43], gametogenesis [44]. Notably, m^6A modification plays a crucial role in the regulation of reproductive process. However, the role of m^6A methylation in the development process of Zi geese small yellow follicle remains elusive. In the present study, the expression levels of m^6A methylation enzymes in small yellow follicle tissues from the HSYF and ASYF groups were detected. We found that the m^6A methylation enzyme *METTL14* and *IGF2BP1* expression level in HSYF group was significantly lower compared to ASYF group, while *YTHDF2* expression level produced the opposite results. This study further supports a strongly correlation between m^6A methylation enzyme and small yellow follicle growth. Hence, In our study, we put emphasized on the genetic differences in small yellow follicle development between high yield and low egg yield of Zi geese from an epigenetic perspective for the first time. In the present study, we performed methylated RNA immunoprecipitation sequencing on small yellow follicle tissues of Zi geese to mine and identify differentially expressed methylated genes. we found that m^6A methylation was more widely distributed in small yellow follicle tissues of Zi geese, and the m^6A peaks located in stop codon regions were the most prominent, indicating translational regulation play a critical role in follicle development of Zi geese. The enrichment of m^6A peaks in stop codon regions of small yellow follicles

are consistent with previous studies on poultry reproductive tissues [19,20,45], supporting the canonical m⁶A modification pattern in folliculogenesis. Compared to the HSYF group, 1174 upregulated m⁶A peaks and 1250 downregulated m⁶A peaks were observed in the ASYF group, these differential peaks covered gene related to follicle development, such as BMP5, METTL14, NGF, PPARGC1A and WTAP. NGF, as a neurotrophin, has been demonstrated to involved in reproduction physiology, including follicle development, oocyte maturation and ovulation [46]. It has been demonstrated that NGF activates the PI3K/AKT signaling pathway via METTL14, which regulates testosterone synthesis of porcine theca cells [47]. PPARGC1A is considered as a powerful coactivator of many transcriptional factors, which is involved in granulosa cell apoptosis of goat [48]. It is noteworthy that nitric oxide may be upregulaed the mRNA expression of PPARGC1A and its downstream through cGMP pathway, and participate in regulating the granulosa cell steroidogenesis through mitochondrial dependent pathway [49]. Hence, we speculated that PPARGC1A plays a vital role in the development of granulosa cell. Previous studies have suggested that overexpression of TGFβ2 could inhibit the proliferation and differentiation of GCs. The bone morphogenetic protein (BMP) family is composed of multiple growth factor proteins belonging to the transforming growth factor-β (TGF-β) superfamily [50], further implying the importance of TGFβ2 in goose follicle development [51]. The bone morphogenetic protein 5 (BMP5) has been shown to be involved in hierarchical follicle development in the early stage of goose [52]. In our study, these DMGs are involved in various important pathways, such as focal adhesion, lysine degradation, and ECM receptor interaction pathway. It has been found that the ECM receptor interaction and the TGFβ signaling were proven to participate in regulating ovarian functiona at Yao shan chicken [53]. Interestingly, focal adhension serve as binding sites for integrins that engage with the surrounding extracellular matrix (ECM) [54]. this findings further supports that these critical pathways plays a regulatory role in regulating follicle growth and development of Zi goose. Lysine is typically the first or second limiting amino acid in poultry diets, which functions as a substrate for protein synthesis [55,56]. Previous studies have suggested that dietary with lysine affected the concentration of FSH in plasma of breeder hens [57]. This findings imply that the lysine degradation signaling pathway may be maintain normal follicular development by influencing the secretion of reproductive hormones during the process of follicular development.

To further explore the critical role of m⁶A modification in regulating the growth and development of small yellow follicles in Zi geese. We performed integrated analysis of RNA-seq and MeRIP-seq data. In the present study, we found that most of the identified DEGs exhibited m⁶A methylation modifications across their mRNA transcripts. The Go and KEGG enrichment of DMGs in the present study was several signaling pathways associated with the follicles development, including neuroactive ligand receptor interaction, mTOR signaling pathway, ECM receptor ineration, Wnt signaling pathway, Notch signaling pathway, TGFβ signaling pathway, and ubiquitin mediated proteolysis. Recent evidence has demonstrated that neuroactive ligand -receptor interaction pathway are involved in the ovarian development of Ninghai indigenou chickens across different egg-laying stages [58]. Treament of chicken granulosa cell with mTOR agonist MHY1485 enhanced granulosa cell proliferation and inhibited apoptosis [59], suggesting that mTOR signaling is involved in regulation of follicular development in aged laying hens. Wnt inhibitor factor 1(WIF1) modulates GCs development by suppressing the Wnt/β-catenin signaling pathway [60]. These findings reveal that the signaling pathway enriched by DMGs closely related to follicular granulosa cell development.

As a core component of the m⁶A methyltransferase complex, METTL14 is capable of acting as a structural scaffold for the entire RNA methyltransferase complex [61,62]. METTL3/METTL14 has been played a pivotal role in a variety of reproduction processes, such as spermatogenesis [63], premature ovarian failure [24], gametogenesis [64]. In current study, MeRIP sequencing was performed to identify the potential genes associated with goose ovarian follicle development. In particular, METTL14 was identified as a key reproductive gene through MeRIP sequencing experimental technique. Herein, this study focused on the function of METTL14 in goose follicular

granulosa cells. We found that overexpression of METTL14 can significantly inhibited the proliferation and promoted the apoptosis of GCs via cell proliferation and apoptosis assays, whereas knockdown of METTL14 led to the opposite biological effects compared with overexpression METTL14, indicating that METTL14 may function as a key regulator in granulosa cell proliferation, apoptosis during goose follicular development. Previous studies have demonstrated that ovarian follicle development is driven by the proliferation and differentiation of granulosa cells, dysregulation of cell cycle transition impair granulosa cell proliferation and differentiation, leading to follicular atresia [65,66]. In this study, we found that knockdown of METTL14 significantly increase the protein expression level of cell apoptosis genes, including PCNA, BCL2, as well as decrease the protein protein expression of anti-apoptosis genes including BAX, Caspase 3 and Caspase 8. Additionally, knockdown of METTL14 promotes the cell cycle progression from S to G2/M phase, suggesting METTL14 may serve as an important regulator that affect the procession of cell cycle in Zi geese follicular granulosa cells, which determined the fate of granulosa cell development.

Follicle development in poultry is complex and highly coordinated physiological process that is precisely regulated by endocrine hormones, especially steroid hormones [60,67]. Progesterone and estradiols are mainly synthesized by follicular granulosa and theca cells, are critical for follicle recruitment, selection and ovulation [68,69]. Among them, these reproductive hormones feedback to the pituitary to influencing the secretion of FSH and LH [70]. Coordinated effects of FSH and LH are essential for normal follicular growth, maturation and ovulation [29]. The present study that knockdown of METTL14 significantly promotes the synthesis of FSH, LH and P4 of GCs. In the meantime, knockdown of METTL14 significantly upregulated the mRNA expression level of StAR, CYP11A1, CYP19A1 and CYP17A1 in GCs as determined by RT-qPCR, which was further confirmed by western blotting at the protein level. This findings collectively suggest that METTL14 has the potential to regulate goose follicle development by influencing the secretion level of steroid hormone and the mRNA expression level of steroidogenic enzymes of GCs.

It has been shown that oxidative stress inhibits follicle granulosa cell proliferation, and promotes apoptosis and autophagy, which further trigger follicular atresia [71,72]. The present study that knockdown of METTL14 increase the content of SOD, CAT, GSH in GCs, as well as decrease the content of MDA in GCs, while overexpression of METTL14 causes opposite effects, suggesting that METTL14 may be considered as an important key molecules, which alleviate follicular atresia caused by oxidative stress in Zi geese. However the specific molecular mechanism by which METTL14 mediated m⁶A methylation regulated the development of follicular granulosa cell in Zi geese remains to be further explored.

5. Conclusions

Taken together, this study revealed that m⁶A methylation modification was widely distributed in small yellow follicle tissue of Zi geese. A total of 78 DMGs were identified in ASYF group in relative to HSYF groups, including BMP5, SCD5, PPARGC1A, METTL14, IGF2BP1, and NGF. These DMGs were enriched in pathway associated with follicular development and steroid synthesis, such as TGF β signaling pathway, PPAR signaling pathway, ECM receptor interaction, neuroactive ligand receptor interaction, Wnt signaling pathway. By integrating the data results of MeRIP-seq and RNA-seq analyses, we demonstrated that METTL14 plays a pivotal role in regulating ovarian follicular development and egg production performance. Mechanistically, our findings indicated that knockdown of METTL14 may exert profound effects on granulosa cell development by promoting GCs steroid hormone synthesis, cell proliferation, inhibiting GCs apoptosis, and maintaining oxidative stress balance (Figure 19). These findings provide a novel insights into the epigenetic regulatory mechanisms of m⁶A methylation modification in follicular growth, development in Zi geese, and offer a theoretical foundation for breeding of geese with high laying performance.

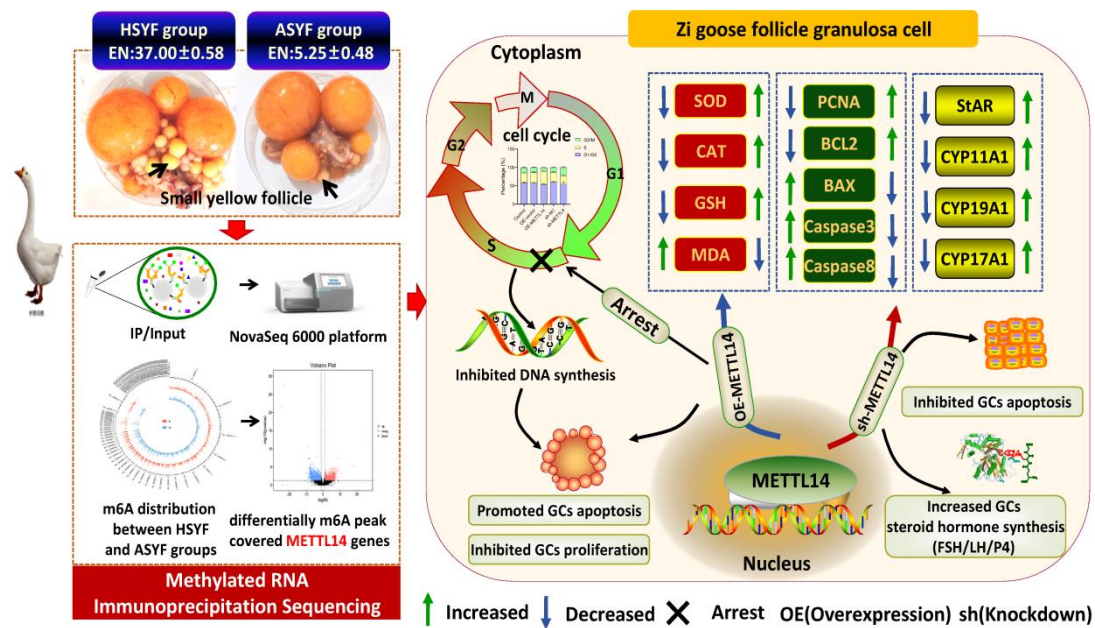


Figure 19. Identification of differentially expressed methylation genes associated with egg production traits via MeRIP-seq and RNA-seq analyse in small yellow follicle of Zi geese; Effect of *METTL14* knockdown and overexpression on follicular granulosa cell development of Zi geese. Red arrows referred as increase, Blue arrow referred as decrease.

Author: contributions: Conceptualization, B.Z. and F.C.; Methodology, Q.D., G.M and K.Y; Formal analysis, L.F. and D.W.; Investigation, B.W. and D.H.; Data Curation, H.Z. and J.Z.; Writing-original draft preparation, B.Z.; Writing-review and editing, F.C. and B.Z.; Supervision, D.H., and X.H.; Funding acquisition, B.Z and F.C. All authors have read and agreed to the published version of the manuscript.

Funding: This: research was supported by Heilongjiang Provincial Finance Department Youth Project for Basic Operational funds of Provincial Research Institutes (CZKYF2025-1-C018); Progesterone Synthesis and Secretion Mechanism in Follicular Granulosa Cell of Herbivorous Livestock and Poultry; China Agriculture Research System (CARS-42-34).

Institutional Review Board Statement: All animal procedures in this study were approved by Institutional Animal Care and Use Committee of Heilongjiang Academy of Agricultural Sciences (HAAS20140025).

Data availability Sataments: The data supporting the conclusion of this article will be made available by the authors, without undue reservation.

Acknowledgments: We thank all members in our research group for their technical assistance and helpful discussions during the experiment.

Conflicts of Interest: The authors have declared that no competing interests exist.

Abbreviations

The following abbreviations are used in this manuscript:

HSYF	Healthy Small Yellow Follicle
ASYF	Atresia Small Yellow Follicle
FSHR	Follicle Stimulating Hormone
CYP11A1	Cytochrome P450 Family 11 Subfamily A member 1
CYP19A1	Cytochrome P450 Family 19 Subfamily A member
CYP17A1	Cytochrome P450 Family 17 Subfamily A member 1
StAR	Steroidogenic Acute Regulatory Protein

FTO	Fat Mass and Obesity Associated
METTL14	methyltransferase 14
WTAP	WT1 Associated Protein
IGF2BP3	Insulin Like Growth Factor 2 mRNA Binding Protein 3
ALKBH5	Alkylation Repair Homolog Protein 5
YTHDF1	YTH Domain Family, Member 1
YTHDF2	YTH Domain Family, Member 2
YTHDF3	YTH domain family, member 3
BMP5	Bone Morphogenetic Protein 5
PPARGC1A	PPARG Coactivator 1alpha
NGF	Nerve Growth Factor; SCD5: Stearoyl-CoA desaturase 5
MeRIP-seq	Methylated RNA Immunoprecipitation Sequencing
RNA-seq	RNA sequencing

References

1. Zhao, H.; Sun, G.; Mu, X.; Li, X.; Wang, J.; Zhao, M.; Zhang, G.; Ji, R.; Chen, C.; Gao, G., et al. Genome-wide selective signatures mining the candidate genes for egg laying in goose. *BMC Genomics* **2023**, *24* (1), 750.
2. Ni, H.; Zhang, Y.; Yang, Y.; Yin, Y.; Ren, J.; Xiao, Q.; Zhao, P.; Hong, X.; Zhang, Z.; Cui, B., et al. Integrated analysis of whole genome and transcriptome sequencing uncovers genetic differences between Zi goose and Xianghai flying goose. *Anim. Genet.* **2024**, *55* (1), 147-151.
3. Sun, X.; Chen, X.; Zhao, J.; Ma, C.; Yan, C.; Liswaniso, S.; Xu, R.; Qin, N. Transcriptome comparative analysis of ovarian follicles reveals the key genes and signaling pathways implicated in hen egg production. *BMC Genomics* **2021**, *22* (1), 899.
4. Chen, Q.; Wang, Y.; Liu, Z.; Guo, X.; Sun, Y.; Kang, L.; Jiang, Y. Transcriptomic and proteomic analyses of ovarian follicles reveal the role of VLDLR in chicken follicle selection. *BMC Genomics* **2020**, *21* (1), 486.
5. Li, D.; Ning, C.; Zhang, J.; Wang, Y.; Tang, Q.; Kui, H.; Wang, T.; He, M.; Jin, L.; Li, J., et al. Dynamic transcriptome and chromatin architecture in granulosa cells during chicken folliculogenesis. *Nat. Commun.* **2022**, *13* (1), 131.
6. Zhang, W.; Chen, X.; Guo, A.; Zhao, Z.; Zhang, B.; Li, F.; Zhang, H. IGF2/IGFBP4 reduces apoptosis and increases free cholesterol of chicken granulosa cells in vitro. *Poult. Sci.* **2024**, *103* (12), 104416.
7. Zheng, Z.; Zuo, W.; Ye, R.; Grunberger, J. W.; Khurana, N.; Xu, X.; Ghandehari, H.; Chen, F. Silica Nanoparticles Promote Apoptosis in Ovarian Granulosa Cells via Autophagy Dysfunction. *Int. J. Mol. Sci.* **2023**, *24* (6).
8. Li, Z.; Ruan, Z.; Feng, Y.; Wang, Y.; Zhang, J.; Lu, C.; Shi, D.; Lu, F. METTL3-mediated m6A methylation regulates granulosa cells autophagy during follicular atresia in pig ovaries. *Theriogenology* **2023**, *201*, 83-94.
9. Liu, X.; Wang, H.; Zhao, X.; Luo, Q.; Wang, Q.; Tan, K.; Wang, Z.; Jiang, J.; Cui, J.; Du, E., et al. Arginine methylation of METTL14 promotes RNA N(6)-methyladenosine modification and endoderm differentiation of mouse embryonic stem cells. *Nat. Commun.* **2021**, *12* (1), 3780.
10. Abakir, A.; Giles, T. C.; Cristini, A.; Foster, J. M.; Dai, N.; Starczak, M.; Rubio-Roldan, A.; Li, M.; Eleftheriou, M.; Crutchley, J., et al. N(6)-methyladenosine regulates the stability of RNA:DNA hybrids in human cells. *Nat. Genet.* **2020**, *52* (1), 48-55.
11. Li, Q.; Shen, H.; Liu, A.; Yu, L.; Wang, L.; Zhang, X. FTO-mediated m6A modification elevates the MFN2 mRNA stability to suppress ovarian granulosa cell senescence. *Int. J. Biol. Macromol.* **2025**, *307* (Pt 4), 142181.
12. Oerum, S.; Meynier, V.; Catala, M.; Tisé, C. A comprehensive review of m6A/m6Am RNA methyltransferase structures. *Nucleic Acids Res.* **2021**, *49* (13), 7239-7255.
13. He, P. C.; Wei, J.; Dou, X.; Harada, B. T.; Zhang, Z.; Ge, R.; Liu, C.; Zhang, L. S.; Yu, X.; Wang, S., et al. Exon architecture controls mRNA m(6)A suppression and gene expression. *Science* **2023**, *379* (6633), 677-682.
14. Wang, X.; Zhao, B. S.; Roundtree, I. A.; Lu, Z.; Han, D.; Ma, H.; Weng, X.; Chen, K.; Shi, H.; He, C. N(6)-methyladenosine Modulates Messenger RNA Translation Efficiency. *Cell* **2015**, *161* (6), 1388-1399.
15. Jiang, X.; Liu, B.; Nie, Z.; Duan, L.; Xiong, Q.; Jin, Z.; Yang, C.; Chen, Y. The role of m6A modification in the biological functions and diseases. *Signal Transduct Target Ther* **2021**, *6* (1), 74.

16. Zhang, M.; Wu, X.; Guo, T.; Xia, Y.; Wang, Z.; Shi, Z.; Hu, K.; Zhu, X.; Zhu, R.; Yue, Y., et al. Involvement of METTL3-mediated m6A methylation in the early development of porcine cloned embryos. *Theriogenology* **2024**, *226*, 378-386.
17. Chen, Y.; Wang, J.; Xu, D.; Xiang, Z.; Ding, J.; Yang, X.; Li, D.; Han, X. m(6)A mRNA methylation regulates testosterone synthesis through modulating autophagy in Leydig cells. *Autophagy* **2021**, *17* (2), 457-475.
18. Liu, K.; Zhou, X.; Li, C.; Shen, C.; He, G.; Chen, T.; Cao, M.; Chen, X.; Zhang, B.; Chen, L. YTHDF2 as a Mediator in BDNF-Induced Proliferation of Porcine Follicular Granulosa Cells. *Int. J. Mol. Sci.* **2024**, *25* (4).
19. Zhang, Y.; Chen, Y.; Ji, H.; Niu, Y.; He, L.; Wang, W.; Yu, T.; Han, R.; Tian, Y.; Liu, X., et al. Dynamic m(6)A Modification Landscape During the Egg Laying Process of Chickens. *Int. J. Mol. Sci.* **2025**, *26* (4).
20. Fan, Y.; Zhang, C.; Zhu, G. Profiling of RNA N6-methyladenosine methylation during follicle selection in chicken ovary. *Poult. Sci.* **2019**, *98* (11), 6117-6124.
21. Guo, S.; Wang, X.; Cao, M.; Wu, X.; Xiong, L.; Bao, P.; Chu, M.; Liang, C.; Yan, P.; Pei, J., et al. The transcriptome-wide N6-methyladenosine (m(6)A) map profiling reveals the regulatory role of m(6)A in the yak ovary. *BMC Genomics* **2022**, *23* (1), 358.
22. Guo, Z.; Shafik, A. M.; Jin, P.; Wu, Z.; Wu, H. Detecting m6A methylation regions from Methylated RNA Immunoprecipitation Sequencing. *Bioinformatics* **2021**, *37* (18), 2818-2824.
23. Huang, E.; Chen, L. RNA N(6)-methyladenosine modification in female reproductive biology and pathophysiology. *Cell Commun Signal* **2023**, *21* (1), 53.
24. Chen, J.; Fang, Y.; Xu, Y.; Sun, H. Role of m6A modification in female infertility and reproductive system diseases. *Int. J. Biol. Sci.* **2022**, *18* (9), 3592-3604.
25. Wang, Y.; Yang, C.; Sun, H.; Jiang, H.; Zhang, P.; Huang, Y.; Liu, Z.; Yu, Y.; Xu, Z.; Xiang, H., et al. The Role of N6-methyladenosine Modification in Gametogenesis and Embryogenesis: Impact on Fertility. *Genomics Proteomics Bioinformatics* **2024**, *22* (4).
26. Gilbert, A. B.; Evans, A. J.; Perry, M. M.; Davidson, M. H. A method for separating the granulosa cells, the basal lamina and the theca of the preovulatory ovarian follicle of the domestic fowl (*Gallus domesticus*). *J. Reprod. Fertil.* **1977**, *50* (1), 179-181.
27. Yu, C.; Qiu, M.; Yin, H.; Zhang, Z.; Hu, C.; Jiang, X.; Du, H.; Li, Q.; Li, J.; Xiong, X., et al. miR-138-5p promotes chicken granulosa cell apoptosis via targeting SIRT1. *Anim. Biotechnol.* **2023**, *34* (7), 2449-2458.
28. Zhang, B. B.; Li, X. N.; Li, M. X.; Sun, Y. Y.; Shi, Y. X.; Ma, T. H. miR-140-3p promotes follicle granulosa cell proliferation and steroid hormone synthesis via targeting AMH in chickens. *Theriogenology* **2023**, *202*, 84-92.
29. Nie, R.; Tian, H.; Zhang, W.; Li, F.; Zhang, B.; Zhang, H. NR5A1 and NR5A2 regulate follicle development in chicken (*Gallus gallus*) by altering proliferation, apoptosis, and steroid hormone synthesis of granulosa cells. *Poult. Sci.* **2024**, *103* (5), 103620.
30. Cao, Z.; Zhang, D.; Wang, Y.; Tong, X.; Avalos, L. F. C.; Khan, I. M.; Gao, D.; Xu, T.; Zhang, L.; J. G. K., et al. Identification and functional annotation of m6A methylation modification in granulosa cells during antral follicle development in pigs. *Anim. Reprod. Sci.* **2020**, *219*, 106510.
31. Begum, I. A. Oxidative stress: Oocyte quality and infertility. *Reprod. Toxicol.* **2025**, *137*, 109011.
32. Wang, X.; Yang, J.; Li, H.; Mu, H.; Zeng, L.; Cai, S.; Su, P.; Li, H.; Zhang, L.; Xiang, W. miR-484 mediates oxidative stress-induced ovarian dysfunction and promotes granulosa cell apoptosis via SESN2 downregulation. *Redox Biol* **2023**, *62*, 102684.
33. Zheng, Y.; Qiu, Y.; Wang, Q.; Gao, M.; Cao, Z.; Luan, X. ADPN Regulates Oxidative Stress-Induced Follicular Atresia in Geese by Modulating Granulosa Cell Apoptosis and Autophagy. *Int. J. Mol. Sci.* **2024**, *25* (10).
34. Zhao, X.; Mei, Z.; Li, H.; Wu, Y.; Pan, L.; Cao, Y. Genome-wide association study and candidate gene analysis of reproductive traits in Yili geese. *Poult. Sci.* **2025**, *104* (6), 105127.
35. Han, C.; Zhu, L.; Wang, M.; Hu, J.; Yang, Q.; Liu, Z.; Zhou, Z.; Li, C.; Hou, S.; Cai, W. Genetic parameters and genomic prediction of egg production traits in ducks. *Poult. Sci.* **2025**, *104* (10), 105510.
36. Wadood, A. A.; Wang, J.; Pu, L.; Shahzad, Q.; Waqas, M.; Liu, X.; Xie, L.; Yu, L.; Chen, D.; Akhtar, R. W., et al. Proteomic Analysis Identifies Potential Markers for Chicken Primary Follicle Development. *Animals (Basel)* **2021**, *11* (4).

37. Zhong, C.; Liu, Z.; Qiao, X.; Kang, L.; Sun, Y.; Jiang, Y. Integrated transcriptomic analysis on small yellow follicles reveals that sox21 ankyrin repeat domain family member A inhibits chicken follicle selection. *Anim. Biosci.* **2021**, *34* (8), 1290-1302.
38. Pan, B.; Chai, J.; Fei, K.; Zheng, T.; Jiang, Y. Dynamic changes in the transcriptome and metabolome of pig ovaries across developmental stages and gestation. *BMC Genomics* **2024**, *25* (1), 1193.
39. Dou, Y. D.; Zhao, H.; Huang, T.; Zhao, S. G.; Liu, X. M.; Yu, X. C.; Ma, Z. X.; Zhang, Y. C.; Liu, T.; Gao, X., et al. STMN1 Promotes Progesterone Production Via StAR Up-regulation in Mouse Granulosa Cells. *Sci. Rep.* **2016**, *6*, 26691.
40. Wang, H.; Han, J.; Zhang, X. A. Interplay of m6A RNA methylation and gut microbiota in modulating gut injury. *Gut Microbes* **2025**, *17* (1), 2467213.
41. Yang, Y.; Zheng, Z. m6A Methylation Modification: Perspectives on the Early Reproduction of Females. *Biomolecules* **2025**, *15* (8).
42. Li, D.; Liu, Z.; Zhu, M.; Yu, W.; Mao, W.; Mao, D.; Wang, F.; Wan, Y. Histone lactylation regulates early embryonic development through m6A methyltransferase METTL3 in goats. *Int. J. Biol. Macromol.* **2025**, *309* (Pt 3), 142858.
43. Chen, Z.; Chen, Z.; Mo, J.; Chen, Y.; Chen, L.; Deng, C. m6A RNA methylation modulates autophagy by targeting Map11c3b in bisphenol A induced Leydig cell dysfunction. *J. Hazard. Mater.* **2025**, *485*, 136748.
44. Yang, W.; Zhao, Y.; Yang, Y. Dynamic RNA methylation modifications and their regulatory role in mammalian development and diseases. *Sci. China:Life Sci.* **2024**, *67* (10), 2084-2104.
45. Li, J.; Zhang, X.; Wang, X.; Sun, C.; Zheng, J.; Li, J.; Yi, G.; Yang, N. The m6A methylation regulates gonadal sex differentiation in chicken embryo. *J. Anim. Sci. Biotechnol.* **2022**, *13* (1), 52.
46. Maranesi, M.; Boiti, C.; Zerani, M. Nerve Growth Factor (NGF) and Animal Reproduction. *Adv. Exp. Med. Biol.* **2021**, *1331*, 277-287.
47. Luo, Y.; Zhao, Y.; Zhang, B.; Chen, T.; Chen, X.; Shen, C.; He, G.; Cao, M.; Chen, L.; Wang, Y., et al. METTL14 mediates nerve growth factor-stimulated testosterone synthesis in porcine theca cells†. *Biol. Reprod.* **2024**, *111* (3), 655-666.
48. Zhang, G. M.; An, S. Y.; El-Samahy, M. A.; Zhang, Y. L.; Wan, Y. J.; Wang, Z. Y.; Xiao, S. H.; Meng, F. X.; Wang, F.; Lei, Z. H. Suppression of miR-1197-3p attenuates H₂O₂-induced apoptosis of goat luteinized granulosa cells via targeting PPARGC1A. *Theriogenology* **2019**, *132*, 72-82.
49. Guo, Y. X.; Zhang, G. M.; Yao, X. L.; Tong, R.; Cheng, C. Y.; Zhang, T. T.; Wang, S. T.; Yang, H.; Wang, F. Effects of nitric oxide on steroidogenesis and apoptosis in goat luteinized granulosa cells. *Theriogenology* **2019**, *126*, 55-62.
50. Rossi, R. O.; Costa, J. J.; Silva, A. W.; Saraiva, M. V.; Van den Hurk, R.; Silva, J. R. The bone morphogenetic protein system and the regulation of ovarian follicle development in mammals. *Zygote* **2016**, *24* (1), 1-17.
51. Zhang, W.; Chen, X.; Nie, R.; Guo, A.; Ling, Y.; Zhang, B.; Zhang, H. Single-cell transcriptomic analysis reveals regulative mechanisms of follicular selection and atresia in chicken granulosa cells. *Food Res. Int.* **2024**, *198*, 115368.
52. Wei, C.; Chen, X.; Peng, J.; Yu, S.; Chang, P.; Jin, K.; Geng, Z. BMP4/SMAD8 signaling pathway regulated granular cell proliferation to promote follicle development in Wanxi white goose. *Poult. Sci.* **2023**, *102* (1), 102282.
53. Miao, X.; Wu, T.; Pan, H.; Zhang, Y.; Liu, J.; Fan, Y.; Du, L.; Gong, Y.; Li, L.; Huang, T., et al. Integrative analysis of the ovarian metabolome and transcriptome of the Yaoshan chicken and its improved hybrids. *Front. Genet.* **2024**, *15*, 1416283.
54. Kuo, J. C. Mechanotransduction at focal adhesions: integrating cytoskeletal mechanics in migrating cells. *J. Cell. Mol. Med.* **2013**, *17* (6), 704-712.
55. Khwatenge, C. N.; Kimathi, B. M.; Nahashon, S. N. Transcriptome Analysis and Expression of Selected Cationic Amino Acid Transporters in the Liver of Broiler Chicken Fed Diets with Varying Concentrations of Lysine. *Int. J. Mol. Sci.* **2020**, *21* (16).
56. Macelline, S. P.; Toghyani, M.; Chrystal, P. V.; Selle, P. H.; Liu, S. Y. Amino acid requirements for laying hens: a comprehensive review. *Poult. Sci.* **2021**, *100* (5), 101036.

57. Wang, Y.; Wang, Q.; Yao, X.; Gou, Z.; Lin, X.; Luo, Q.; Jiang, S. Effects and interactions of dietary lysine and apparent nitrogen corrected metabolizable energy on yellow-feathered broiler breeder hens. *J. Anim. Sci. Biotechnol.* **2024**, *15* (1), 143.
58. Huang, X.; Zhou, W.; Cao, H.; Zhang, H.; Xiang, X.; Yin, Z. Ovarian Transcriptomic Analysis of Ninghai Indigenous Chickens at Different Egg-Laying Periods. *Genes (Basel)* **2022**, *13* (4).
59. Hao, E. Y.; Wang, D. H.; Chen, Y. F.; Zhou, R. Y.; Chen, H.; Huang, R. L. The relationship between the mTOR signaling pathway and ovarian aging in peak-phase and late-phase laying hens. *Poult. Sci.* **2021**, *100* (1), 334-347.
60. Nie, R.; Zhang, W.; Tian, H.; Li, J.; Ling, Y.; Zhang, B.; Zhang, H.; Wu, C. Regulation of Follicular Development in Chickens: WIF1 Modulates Granulosa Cell Proliferation and Progesterone Synthesis via Wnt/ β -Catenin Signaling Pathway. *Int. J. Mol. Sci.* **2024**, *25* (3).
61. Liu, X.; Du, Y.; Huang, Z.; Qin, H.; Chen, J.; Zhao, Y. Insights into roles of METTL14 in tumors. *Cell Prolif.* **2022**, *55* (1), e13168.
62. Wang, P.; Doxtader, K. A.; Nam, Y. Structural Basis for Cooperative Function of Mettl3 and Mettl14 Methyltransferases. *Mol. Cell* **2016**, *63* (2), 306-317.
63. Lin, Z.; Hsu, P. J.; Xing, X.; Fang, J.; Lu, Z.; Zou, Q.; Zhang, K. J.; Zhang, X.; Zhou, Y.; Zhang, T., et al. Mettl3-/Mettl14-mediated mRNA N(6)-methyladenosine modulates murine spermatogenesis. *Cell Res.* **2017**, *27* (10), 1216-1230.
64. Fang, F.; Wang, X.; Li, Z.; Ni, K.; Xiong, C. Epigenetic regulation of mRNA N6-methyladenosine modifications in mammalian gametogenesis. *Mol. Hum. Reprod.* **2021**, *27* (5).
65. Ma, X.; Han, X.; Wang, W.; Zhang, Q.; Tang, H. β -Catenin regulates ovarian granulosa cell cycle and proliferation in laying hens by interacting with TCF4. *Poult. Sci.* **2024**, *103* (3), 103377.
66. Li, X.; Luo, X.; Zhang, X.; Guo, Y.; Cheng, L.; Cheng, M.; Tang, S.; Gong, Y. COL1A1 promotes cell proliferation, cell cycle progression, and anoikis resistance in granulosa cells of chicken pre-ovulatory follicles. *Int. J. Biol. Macromol.* **2025**, *306* (Pt 2), 141524.
67. Tang, Y.; Lin, Z.; Liu, L.; Yin, L.; Zhang, D.; Yu, C.; Yang, C.; Gong, Y.; Wang, Y.; Liu, Y. Attenuated AKT signaling by miR-146a-5p interferes with chicken granulosa cell proliferation, lipid deposition and progesterone biosynthesis. *Theriogenology* **2024**, *214*, 370-385.
68. Zhang, D.; Wu, H.; Wang, Y.; Xu, Z.; Sun, X.; Liswaniso, S.; Qin, N.; Xu, R. The inhibition roles of RAB23 gene in granulosa cell proliferation and progesterone synthesis of hen ovarian prehierarchical follicles. *Br. Poult. Sci.* **2024**, *65* (6), 690-698.
69. Li, D.; Li, X.; He, H.; Zhang, Y.; He, H.; Sun, C.; Zhang, X.; Wang, X.; Kan, Z.; Su, Y., et al. miR-10a-5p inhibits chicken granulosa cells proliferation and Progesterone(P4) synthesis by targeting MAPRE1 to suppress CDK2. *Theriogenology* **2022**, *192*, 97-108.
70. Leng, D.; Zeng, B.; Wang, T.; Chen, B. L.; Li, D. Y.; Li, Z. J. Single nucleus/cell RNA-seq of the chicken hypothalamic-pituitary-ovarian axis offers new insights into the molecular regulatory mechanisms of ovarian development. *Zool. Res.* **2024**, *45* (5), 1088-1107.
71. Bao, T.; Yao, J.; Zhou, S.; Ma, Y.; Dong, J.; Zhang, C.; Mi, Y. Naringin prevents follicular atresia by inhibiting oxidative stress in the aging chicken. *Poult. Sci.* **2022**, *101* (7), 101891.
72. Jiang, D.; Wang, X.; Zhou, X.; Wang, Z.; Li, S.; Sun, Q.; Jiang, Y.; Ji, C.; Ling, W.; An, X., et al. Spermidine alleviating oxidative stress and apoptosis by inducing autophagy of granulosa cells in Sichuan white geese. *Poult. Sci.* **2023**, *102* (9), 102879.

Disclaimer/Publisher's Note: The statements, opinions and data contained in all publications are solely those of the individual author(s) and contributor(s) and not of MDPI and/or the editor(s). MDPI and/or the editor(s) disclaim responsibility for any injury to people or property resulting from any ideas, methods, instructions or products referred to in the content.